Synthesis and Structural Characterisation of Dithiocarbamate-stabilised Dimeric Molybdenum(V) Imido Complexes *via* Oxo Substitution Reactions with Organic Isocyanates†

Thérèse A. Coffey, Glyn D. Forster and Graeme Hogarth *
Chemistry Department, University College London, 20 Gordon Street, London WC1H 0AJ, UK

Thermolysis of molybdenum–oxo complexes $[MoO_2(S_2CNEt_2)_2]$ **1**, $[\{MoO(S_2CNEt_2)(\mu\text{-}O)\}_2]$ **2** and $[Mo_2O_2(S_2CNEt_2)_2(\mu\text{-}O)(\mu\text{-}S)]$ **3** with organic isocyanates afforded a range of imido-substituted binuclear molybdenum(V) complexes. Reaction of complex **1** with 1 equivalent of RNCO gave terminally substituted mono(imido) complexes $[Mo_2O(NR)(S_2CNEt_2)_2(\mu\text{-}S)_2]$ **4a**–**4c** (R = Bu^t, 2,6-$Me_2C_6H_3$ or adamant-1-yl) and bridging bis(imido) complexes $[\{MoO(S_2CNEt_2)(\mu\text{-}NR)\}_2]$ **5a** and **5c** (R = Ph or *p*-tolyl). Reaction of complex **2** with an excess of RNCO afforded the tetraimido complex $[\{Mo(NR)(S_2CNEt_2)(\mu\text{-}NR)\}_2]$ **6b** (R = *o*-tolyl) and the bridging ureato complex $[Mo_2(NPh)_2(S_2CNEt_2)_2(\mu\text{-}NPh)\{\mu\text{-}PhNC(O)NPh\}]$ **7a**, while with PhNCO and complex **3** a further ureato complex $[Mo_2(NPh)_2(S_2CNEt_2)_2(\mu\text{-}S)\{\mu\text{-}PhNC(O)NPh\}]$ **7b** resulted. Thermolysis of complex **7a** gave the tetraimido complex $[\{Mo(NPh)(S_2CNEt_2)(\mu\text{-}NPh)\}_2]$ **6a**, a reaction which is reversed in the presence of PhNCO. Acid-catalysed hydrolysis of complex **6b** afforded the bis(imido) complex $[\{MoO(NR)(S_2CNEt_2)\}_2]$ (R = *o*-tolyl) **5b** which upon thermolysis with *o*-tolyl isocyanate regenerated **6b**. Addition of HBF_4 to **5a** resulted in oxo substitution by dithiocarbamate to give $[Mo_2O(S_2CNEt_2)_3(\mu\text{-}NPh)_2][BF_4]$ **8**. Six of these complexes, namely **4a**, **4b**, **5b**, **6b**, **7a** and **8**, have been characterised by X-ray crystallography. All are dimeric and contain relatively short molybdenum–molybdenum contacts (2.625–2.822 Å) indicative of metal–metal bonding, the longer distances being associated with bridging sulfido ligands. Terminal imido ligands are all linear and bridging imido ligands planar.

The chemistry of oxo- and sulfido-containing dimeric molybdenum(V) complexes has been an area of intense interest, primarily since such complexes act as models for metalloenzymes.[1] Perhaps the most studied of complexes of this type are those containing the $[Mo_2X_2(\mu\text{-}X)_2]^{2+}$ core, being stabilised further by the addition of monoanionic, often chelating ligands.[2] For example, dithiocarbamate-[3] and dithiophosphate-stabilised[4] complexes are known for almost all possible combinations of terminal and bridging oxo and sulfido ligands.

Surprisingly then, complexes of this type containing a closely related π-donor moiety, the imido ligand, are rare. The first imido complex containing dithiophosphate ligands, $[\{Mo(NC_6H_4Me\text{-}p)\{S_2P(OEt)_2\}(\mu\text{-}S)\}_2]$, was reported by Edelblut and Wentworth[5] and is formed upon addition of hydrogen sulfide to monomeric $[Mo(NC_6H_4Me\text{-}p)\{S_2P(OEt)_2\}_3]$. The crystal structure of this molybdenum(V) complex revealed, however, that in the solid state, a tetrameric cubane structure was adopted in preference to the expected dimeric structure, dimolybdenum units being linked *via* triply-bridging sulfido ligands.[5] In solution the situation becomes more complicated, with a dimer–tetramer equilibrium being established [equation (1)].

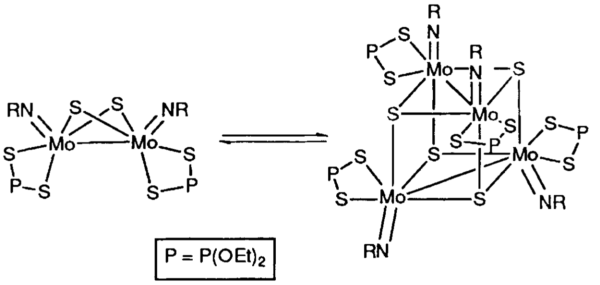

(1)

In order to investigate this equilibrium further, one of the imido ligands was replaced by an oxo moiety, but the resulting complex $[Mo_2O(NC_6H_4Me\text{-}p)\{S_2P(OEt)_2\}_2(\mu\text{-}S)]$ was also found to display similar solution and solid-state properties.[6] Replacement of both imido ligands by oxo moieties, however, pushed the equilibrium over to the dimer, and for $[\{MoO\{S_2P(OEt)_2\}(\mu\text{-}S)\}_2]$ no evidence was found for tetramer formation.[7] Such dimer–tetramer equilibria are not restricted to complexes containing dithiophosphate ligands. Notably, the analogous dithiocarbamate-stabilised bis(imido)-complex $[\{Mo(NC_6H_4Me\text{-}p)(\mu\text{-}S)(\eta^2\text{-}S_2CNPr^i{}_2)\}_n]$ ($n = 2$ or 4) also shows this behaviour, indeed in this instance both dimeric and tetrameric forms have been crystallographically characterised.[8]

The role of the imido ligand in promoting the formation of the tetrameric cubane-like structure is not clear. The added steric requirements of the organic substituent on nitrogen appears to play little part since it faces away from the second dimer molecule. The better π-donor properties of the imido *versus* oxo or sulfido ligand may be important, the increase in electron density at the metal centre being relayed to the sulfido ligands which become more basic. Indeed this appears to be the case, since while $[\{MoO\{S_2P(OEt)_2\}(\mu\text{-}S)\}_2]$ is unaffected by trifluoroacetic acid, a bridging sulfido ligand in $[\{Mo(NC_6H_4Me\text{-}p)\{S_2P(OEt)_2\}(\mu\text{-}S)\}_n]$ is readily protonated

---

† *Supplementary data available*: see Instructions for Authors, *J. Chem. Soc., Dalton Trans.*, 1995, Issue 1, pp. xxv–xxx.

yielding $[Mo_2(NC_6H_4Me\text{-}p)_2\{S_2P(OEt)_2\}(\mu\text{-}SH)(\mu\text{-}S)(\mu\text{-}O_2CCF_3)]$.[9]

It should be noted that in all the complexes discussed above, the imido ligands are bound only to a single metal centre. Indeed, no dithiocarbamate-stabilised complexes of this type are known in which imido ligands bridge the binuclear centre, and one dithiophosphate complex, $[Mo_2O_2\{S_2P(OEt)_2\}(\mu\text{-}O)(\mu\text{-}NH)]$, has been reported.[10] This is surprising since a number of such complexes are known for the closely related cyclopentadienyl-stabilised dimolybdenum centre. For example, the bis- and mono-(imido) complexes $[\{Mo(\eta^5\text{-}C_5H_4Me)O(\mu\text{-}NPh)\}_2]$ and $[Mo_2(\eta^5\text{-}C_5H_4Me)_2O_2(\mu\text{-}O)(\mu\text{-}NPh)]$ have both been shown by X-ray crystallography to contain bridging imido ligands,[11] while in this series of complexes the tetraimido complex $[\{Mo(\eta^5\text{-}C_5H_4Me)(NPh)(\mu\text{-}NPh)\}_2]$ has also been prepared.[12] In these cyclopentadienyl complexes, the imido ligands were introduced *via* substitution of an oxo moiety upon reaction with phenyl isocyanate.[12] The use of organic isocyanates in the synthesis of imido ligands is well documented[12,13] and is often advantageous since many metal–oxo complexes are known, and the carbon dioxide produced is easily removed from the system. The reaction is believed to occur *via* an initial [2 + 2] cycloaddition of the isocyanate to the metal–oxygen bond resulting in the formation of a four-membered metallacycle [equation (2)]. Such an intermediate can break down back to the oxide and isocyanate, or go on to give the imido complex and carbon dioxide. Evidence for a metallacyclic intermediate comes from the reaction of $[Mo(\eta^5\text{-}C_5H_5)_2O]$ with phenyl isocyanate which leads to formation of $[Mo(\eta^5\text{-}C_5H_5)_2\{\eta^2\text{-}PhNC(O)O\}]$ characterised by X-ray crystallography.[14] Interestingly, the latter does not break down to afford the anticipated imido complex upon thermolysis or UV irradiation, which is surprising since such imido complexes have been independently prepared from monocyclopentadienyl precursors.[15] Indeed, while the [2 + 2] cycloaddition mechanism is often cited, and generally accepted, it has yet to be proven.[16]

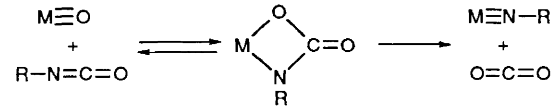

(2)

In light of the above, we considered that well known and readily accessible dithiocarbamate-stabilised molybdenum oxides such as $[MoO_2(S_2CNEt_2)_2]$ **1**,[17] $[\{MoO(S_2CNEt_2)_2(\mu\text{-}O)\}_2]$ **2**[18] and $[Mo_2O_2(S_2CNEt_2)_2(\mu\text{-}O)(\mu\text{-}S)]$ **3**[18] may be useful precursors towards the preparation of both monomeric molybdenum(VI) and dimeric molybdenum(V) imido complexes. This is indeed the case, for example with regard to the former, bis(imido) $[Mo(NR)_2(S_2CNEt_2)_2]$[19] and mono(imido) $[Mo(NR)(\eta^2\text{-}S_2)(S_2CNEt_2)_2]$[20] complexes are readily accessed upon reaction of **1** with organic isocyanates. In these reactions however, a number of dimeric molybdenum(V) complexes were also formed, while with **2** and **3** all complexes produced retained the dimeric molybdenum(V) core. This paper is concerned with these dimeric molybdenum(V) complexes and describes their synthesis, structure and reactivity. Aspects of this work have been communicated previously.[21,22]

Results and Discussion

Terminal Mono(imido) Complexes $[Mo_2O(NR)(S_2CNEt_2)_2(\mu\text{-}S)_2]$ **4**.—Thermolysis of $[MoO_2(S_2CNEt_2)_2]$ **1** with 1 equivalent of the sterically incumbant organic isocyanates (RNCO; R = Bu^t, 2,6-$Me_2C_6H_3$ or adamant-1-yl) for 3 d led to the formation of mono(imido) complexes $[Mo_2O(NR)(S_2CNEt_2)_2(\mu\text{-}S)_2]$ **4a–4c** as air-stable yellow crystalline solids in low yields (4–32%) after chromatography [equation (3)]. Characterisation was relatively straightforward, with all displaying a strong absorption at 972–953 cm^{-1} in the IR spectrum attributed to a terminal metal–oxo moiety, while ^1H NMR spectra indicated a 2 : 1 ratio of dithiocarbamate and imido substituents. While the yellow colouration was indicative of a binuclear as opposed to a tetranuclear cubane type structure,[8] in order to confirm this, X-ray crystallographic studies were carried out on two of the complexes, namely $[Mo_2O(NBu^t)(S_2CNEt_2)_2(\mu\text{-}S)_2]$ **4a** and $[Mo_2O(NC_6H_3Me_2\text{-}2,6)(S_2CNEt_2)_2(\mu\text{-}S)_2]$ **4b**, the results of which are summarised in Figs. 1 and 2 and Tables 1 and 2 respectively.

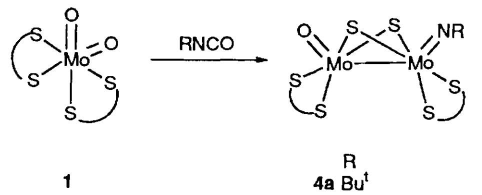

(3)

1

4a Bu^t
4b 2,6-$Me_2C_6H_3$
4c adamantyl

Both molecules are indeed dimeric and consist of two molybdenum(V) centres, with approximate distorted square-

Table 1 Selected bond lengths (Å) and angles (°) for complex **4a**

Mo(1)–Mo(2)	2.822(1)	Mo(1)–S(1)	2.485(2)
Mo(1)–S(2)	2.470(2)	Mo(2)–S(3)	2.491(2)
Mo(2)–S(4)	2.499(2)	Mo(1)–S(5)	2.326(2)
Mo(2)–S(5)	2.336(2)	Mo(1)–S(6)	2.334(2)
Mo(2)–S(6)	2.326(2)	Mo(1)–O(1)	1.670(4)
Mo(2)–N(3)	1.705(4)		
S(1)–Mo(1)–S(2)	70.6(1)	S(3)–Mo(2)–S(4)	69.9(1)
Mo(1)–S(5)–Mo(2)	74.5(1)	Mo(1)–S(6)–Mo(2)	74.5(1)
Mo(2)–Mo(1)–O(1)	106.3(1)	Mo(1)–Mo(2)–N(3)	101.8(1)
Mo(2)–N(3)–C(11)	168.4(4)		

Table 2 Selected bond lengths (Å) and angles (°) for complex **4b**

Mo(1)–Mo(2)	2.806(1)	Mo(1)–S(1)	2.460(1)
Mo(1)–S(2)	2.460(1)	Mo(2)–S(3)	2.480(1)
Mo(2)–S(4)	2.471(2)	Mo(1)–S(5)	2.328(1)
Mo(2)–S(5)	2.313(1)	Mo(1)–S(6)	2.322(1)
Mo(2)–S(6)	2.320(1)	Mo(1)–O(1)	1.663(3)
Mo(2)–N(3)	1.713(3)		
S(1)–Mo(1)–S(2)	70.7(1)	S(3)–Mo(2)–S(4)	70.0(1)
Mo(1)–S(5)–Mo(2)	74.4(1)	Mo(1)–S(6)–Mo(2)	74.4(1)
Mo(2)–Mo(1)–O(1)	103.9(1)	Mo(1)–Mo(2)–N(3)	101.8(1)
Mo(2)–N(3)–C(11)	169.6(3)		

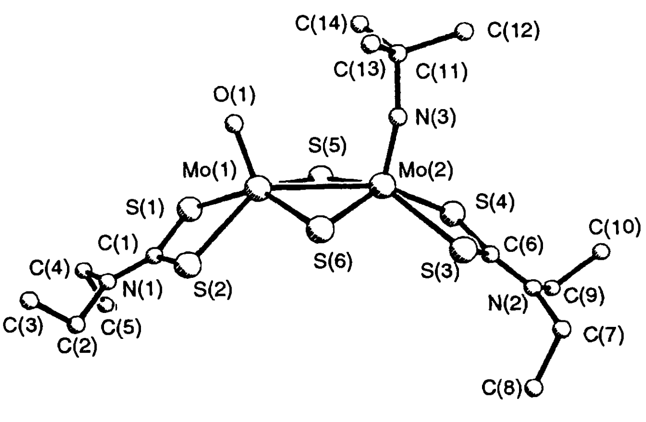

Fig. 1 Molecular structure of complex **4a**

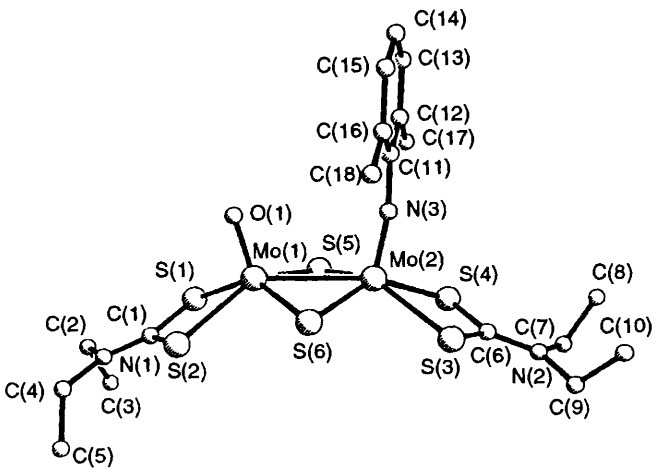

Fig. 2 Molecular structure of complex **4b**

based pyramidal geometry (ignoring the metal–metal bond), in relatively close proximity [Mo(1)–Mo(2) **4a**, 2.822(1); **4b**, 2.806(1) Å]. The dimolybdenum centre is bridged approximately symmetrically by two sulfido moieties, the most significant deviation being 0.015 Å [**4b** Mo(1)–S(5) 2.328(1), Mo(2)–S(5) 2.313(1) Å] which is less than that seen for both sulfido ligands in $[\{Mo(NC_6H_4Me\text{-}p)(\eta^2\text{-}S_2CNPr^i_2)(\mu\text{-}S)\}_2]$($\Delta$ Mo–S_b 0.024 and 0.030 Å).[8] The imido ligands are approximately linear [Mo(2)–N(3)–C(11) **4a**, 168.4(4); **4b**, 169.6(3)°] with the short metal–nitrogen [Mo(2)–N(3) **4a**, 1.705(4); **4b**, 1.713(3) Å] and metal–oxygen [Mo(1)–O(1) **4a**, 1.670(4); **4b**, 1.663(3) Å] contacts being typical.[23] Both molecules show the expected *cis* configuration of dithiocarbamate ligands, and as in related disulfido-bridged complexes,[24] the Mo_2S_2 core is puckered, the dihedral angle between the planes defined by the bridging sulfur atoms and each molybdenum (**4a**, 150.5; **4b**, 146.2°) comparing well with values of 147–153° found previously.

In contrast to those complexes previously reported that contain two bridging sulfido ligands and one[6] or two[8] terminal imido ligands, we could find no evidence of cubane formation for complexes **4a**–**4c**. The arylimido complex **4b** does however form dimers in the solid state *via* a weak interaction between the oxo ligand, O(1), and the one of the nitrogens, N(1), of a dithiocarbamate ligand as shown in Fig. 3. This can be rationalised as an electrostatic attraction between the negatively charged oxo group and the positive charge on the nitrogen which arises from the canonical form of the dithiocarbamate ligand whereby both sulfurs carry a negative charge. The intermolecular interaction also accounts for the rather unusual 'up–up' configuration of the ethyl substituents on the dithiocarbamate ligands in **4b** as opposed to the more normal 'up–down' configuration observed in **4a** and related complexes, since it is only in the former that the two binuclear fragments can lock together without incurring unfavourable steric interactions with other parts of the molecule. That this intermolecular interaction is not observed in **4a** may be a result of the different steric demands of the aryl and alkyl substituents.

The reason for the lack of cubane formation in these complexes is not clear. The presence of imido ligands is known to be important in cubane formation as this behaviour is not observed in analogous complexes containing only terminal oxo or sulfido moieties.[24,25] It should be emphasised that we cannot completely rule out the possibility of a dimer–tetramer equilibrium in these complexes, however since all remain yellow in solution, it must significantly favour the dimer.

The route *via* which these complexes are formed is also unclear. We considered that the unsubstituted complex $[\{MoO(S_2CNEt_2)(\mu\text{-}S)\}_2]$ might be formed initially as a thermal degradation product of **1**, with imido substitution taking place after the reduction. This was discounted since no significant reaction was observed upon thermolysis of $[\{MoO(S_2CNEt_2)(\mu\text{-}S)\}_2]$ with either aryl or alkyl isocyanates. This appears to imply that imido substitution takes place prior to the reduction and dimer formation, however, thermolysis of the mononuclear molybdenum(VI) products of this reaction, namely the bis(imido) complex $[Mo(NC_6H_3Me\text{-}2,6)(S_2CNEt_2)_2]$ and imido–disulfur complexes $[Mo(NR)(S_2CNEt_2)_2(\eta^2\text{-}S_2)]$ (R = Bu^t or 2,6-$Me_2C_6H_3$), did not furnish **4**. Whatever the precise details of this transformation the only source of sulfur is from the dithiocarbamate ligands and this represents another example of the thermal degradation of this generally stable ligand.[20,26]

Table 3 Selected bond lengths (Å) and angles (°) for complex **5b**

Mo(1)–Mo(2)	2.628(1)	Mo(1)–S(1)	2.493(1)
Mo(1)–S(2)	2.461(1)	Mo(2)–S(3)	2.462(1)
Mo(2)–S(4)	2.485(1)	Mo(1)–N(3)	1.962(3)
Mo(2)–N(3)	1.980(3)	Mo(1)–N(4)	1.974(3)
Mo(2)–N(4)	1.960(3)	Mo(1)–O(1)	1.688(3)
Mo(2)–O(2)	1.689(3)		
S(1)–Mo(1)–S(2)	71.0(1)	S(3)–Mo(2)–S(4)	71.0(1)
Mo(1)–N(3)–Mo(2)	83.6(1)	Mo(1)–N(4)–Mo(2)	83.8(1)
Mo(2)–Mo(1)–O(1)	104.8(1)	Mo(1)–Mo(2)–O(2)	105.0(1)

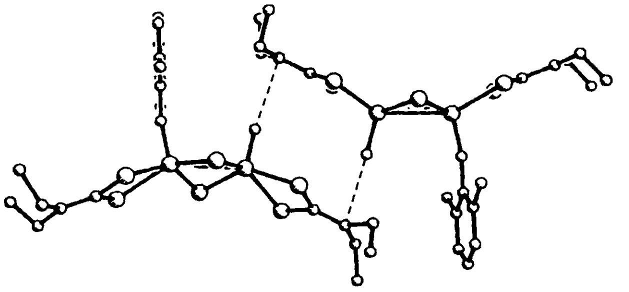

Fig. 3 Interactions between dimeric units in complex **4b**

Bridging Bis(imido) Complexes $[\{MoO(S_2CNEt_2)(\mu\text{-}NR)\}_2]$ **5**.—Thermolysis of less bulky aryl isocyanates (R = Ph or *p*-tolyl) with $[MoO_2(S_2CNEt_2)_2]$ **1** for 3 d led to the formation of bis(imido) complexes $[\{MoO(S_2CNEt_2)(\mu\text{-}NR)\}_2]$ **5a** and **5c** as yellow air-stable crystalline solids in yields of 76 and 50% respectively. While reaction with *o*-tolyl isocyanate did not give **5b** directly, the acid-catalysed hydrolysis of the tetraimido complex $[\{Mo(NC_6H_4Me\text{-}o)(S_2CNEt_2)(\mu\text{-}NC_6H_4Me\text{-}o)\}_2]$ **6b** afforded **5b** in 83% yield [equation (4)]. Identification of **5** as bis(imido) complexes was based on the 1:1 ratio of

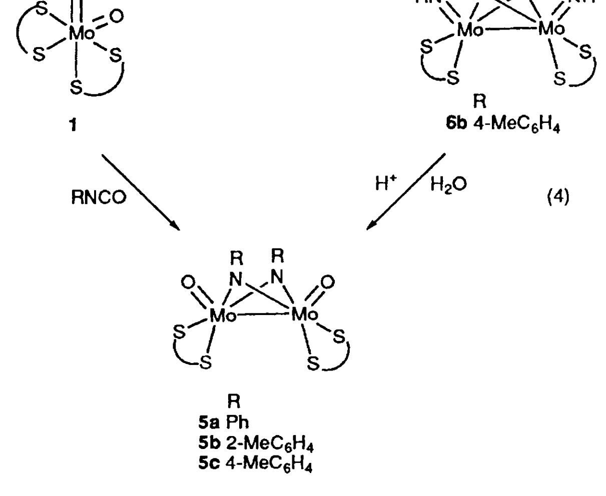

(4)

dithiocarbamate and aryl moieties in the ^1H NMR spectra, while the presence of two terminal oxo ligands was implied from the observation of a pair of intense absorptions in the IR spectra between 950 and 930 cm^{-1}. In order to confirm the spectroscopic formulation an X-ray crystallographic study was carried out on [{MoO(S_2CNEt_2)(μ-NC_6H_4Me-*o*)}$_2$] **5b** the results of which are given in Fig. 4 and Table 3.

The molecule adopts the expected *cis* configuration of dithiocarbamate ligands. The two imido moieties span the dimolybdenum vector approximately symmetrically [Mo(1)–N(3) 1.962(3), Mo(2)–N(3) 1.980(3), Mo(1)–N(4) 1.974(3), Mo(2)–N(4) 1.960(3) Å] with the geometry about each nitrogen being trigonal planar. Each molybdenum also carries a terminal oxo moiety [Mo(1)–O(1) 1.688(3), Mo(2)–O(2) 1.689(3) Å]. As found in the mono(imido) complexes **4**, the central Mo_2X_2 core is puckered, the dihedral angle between the planes containing both bridging nitrogen atoms and each metal atom being 149.2°. The *o*-tolyl rings are orientated approximately perpendicular to the Mo_2N_2 plane, such that the methyl groups point towards the oxo groups and away from the dithiocarbamate ligands, and unlike the tetraimido complex [{Mo(NC_6H_4Me-*o*)(S_2CNEt_2)(μ-NC_6H_4Me-*o*)}$_2$] **6b** (see below), no disorder over the possible *ortho* sites was noted. The molybdenum–molybdenum bond length of 2.628(1) Å is worthy of note since it is significantly shorter than those found in the disulfido-bridged complexes **4a** and **4b**, more closely resembling values found for analogous oxo-bridged complexes, for example [{MoO(S_2CNEt_2)(μ-O)}$_2$] **2** [2.580(1) Å]. The best comparison, however, can be made with the only previously crystallographically characterised imido-bridged complex of this type, [Mo_2O_2{$S_2P(OEt)_2$}$_2$(μ-O)(μ-NH)] [2.589(1) Å].[10] Hence it appears that there is a gradual increase in the molybdenum–molybdenum bond length upon successive replacement of oxo for imido and sulfido bridges.

Unlike the terminal imido complexes **4**, bis(imido) bridged **5a** and **5c** are formed in relatively high yields from the molybdenum(VI) dioxo complex **1**. We again considered that this may be a result of initial formation of [{MoO(S_2CNEt_2)(μ-O)}$_2$] **2** which then undergoes imido substitution, however, thermolysis of **2** with a slight excess of phenyl isocyanate did not afford **5a** but rather led to the isolation of the ureato-bridged complex [$Mo_2(NPh)_2(S_2CNEt_2)_2$(μ-NPh){μ-PhNC(O)NPh}] **7a** (see below). Thus, while **5a** is generated under these conditions, it reacts readily with further isocyanate to afford **7a**, and since the latter was not isolated from the reaction of [$MoO_2(S_2CNEt_2)_2$] **1** with 1 equivalent of phenyl isocyanate, we conclude that the major formation pathway of **5a** is not *via* the intermediacy of **2**. Thus it appears that imido substitution occurs prior to reduction of the metal centre, and we favour a route which involves initial formation of the mono(imido) complex [MoO(NPh)(S_2CNEt_2)$_2$][27] which breaks down *via* loss of tetraethylthiuram disulfide and dimerisation to give **5a** [equation (5)].

The *o*-tolyl derivative [{MoO(NC_6H_4Me-*o*)(S_2CNEt_2)}$_2$] **5b** was not formed upon addition of the isocyanate to **1** or **2**, the tetraimido complex [Mo(NC_6H_4Me-*o*)(S_2CNEt_2)(μ-NC_6H_4-Me-*o*)}$_2$] **6b** being isolated instead (see below). It was however formed in high yield from the acid-catalysed hydrolysis of **6b** which leads to both terminal imido moieties being hydrolysed, while leaving the bridging groups intact. This behaviour has been noted previously for the cyclopentadienyl stabilised tetraimido complex [{Mo(η^5-C_5H_4Me)(NPh)(μ-NPh)}$_2$][12] which is readily hydrolysed in the presence of acid to [{Mo(η^5-C_5H_4Me)O(μ-NPh)}$_2$], while the latter is indefinitely stable in aqueous solutions of concentrated acids.

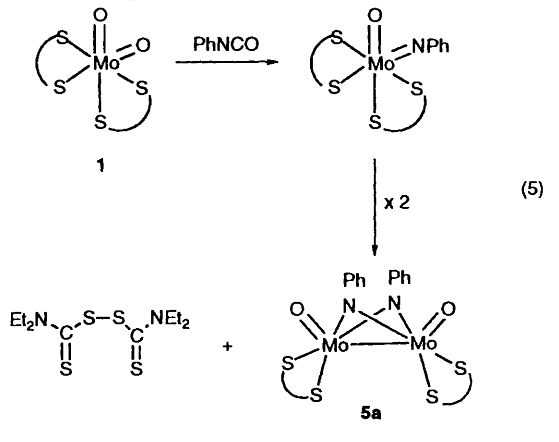

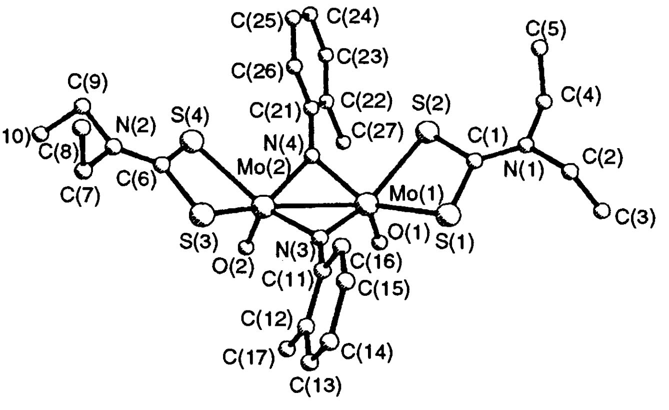

Fig. 4 Molecular structure of complex **5b**

Table 4 Selected bond lengths (Å) and angles (°) for complex **6b**

Mo(1)–Mo(1a)	2.633(1)	Mo(1)–S(1)	2.481(1)
Mo(1)–S(2)	2.493(1)	Mo(1)–N(3)	1.958(3)
Mo(1)–N(3a)	1.978(4)	Mo(1)–N(2)	1.741(3)
S(1)–Mo(1)–S(2)	70.5(1)	Mo(1)–N(3)–Mo(1a)	83.9(1)
N(2)–Mo(1)–Mo(1a)	108.7(1)	Mo(1)–N(2)–C(21)	167.9(3)

Tetraimido Complexes [{Mo(NR)(S_2CNEt_2)(μ-NR)}$_2$] **6**.—Thermolysis of either [$MoO_2(S_2CNEt)_2$] **1** or [{MoO(S_2CNEt_2)(μ-O)}$_2$] **2** with 2–4 equivalents of *o*-tolyl isocyanate affords the tetraimido complex [{Mo(NC_6H_4Me-*o*)(S_2CNEt_2)(μ-NC_6H_4Me-*o*)}$_2$] **6b** as an orange crystalline air-stable solid in yields of 34 and 90% respectively,[22] as does addition of 2 equivalents of the isocyanate to the bis(imido) complex [{MoO(S_2CNEt_2)(μ-NC_6H_4Me-*o*)}$_2$] **5b** (90% yield) [equation (6)]. Complex **6b** was easily characterised on the basis of analytical and spectroscopic data and the formulation was confirmed by an X-ray crystallographic study, the results of which are shown in Fig. 5 and Table 4.

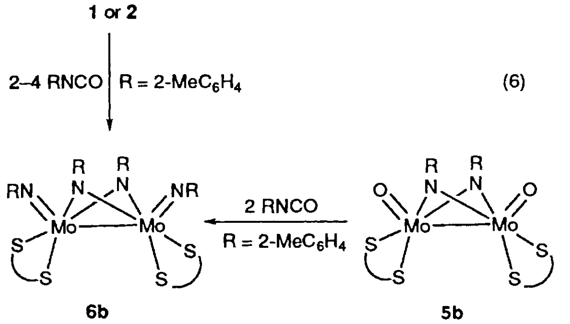

(6)

The molecule is essentially the same as complex **5b**, except that the terminal oxo ligands have been replaced by *o*-tolyl imido groups. This leads to a very slight (but not statistically significant) elongation of the metal–metal vector [Mo(1)–Mo(1a) 2.633(1) Å] and opening up of the Mo_2N_2 core, the dihedral angle between both bridging nitrogens and either molybdenum atom being 149.7°. The terminal imido ligands are similar to those found in **4a** and **4b**, being approximately linear at nitrogen [Mo(1)–N(2)–C(21) 167.9(3)°] and in close contact with the molybdenum centre [Mo(1)–N(2) 1.741(3) Å]. The latter is somewhat longer than the distance of 1.713(3) Å for the metal–imido distance in complex **4b** which may reflect the increased π-donor ability of the 2,6-dimethylphenyl *versus* 2-methylphenyl imido ligand. Another interesting difference between these aryl imido functionalities is the relative orientations of the aryl ring with respect to the metal–metal vector. Thus in **4b**, the plane of the aryl ring lies approximately perpendicular to the metal–metal vector, while in **6b** it is twisted considerably, being closer to parallel with the latter. This appears not to be a consequence of the second methyl substituent since in **6b** the methyl group is disordered over C(22) (shown 60%) and C(26) (40%), while a similar disorder of the bridging sites is also seen.

In solution complex **6b** is fluxional as evidenced by the broad nature of the ^1H NMR spectrum at room temperature in $[^2H_8]$toluene. The fluxional process(es) has been monitored by a variable-temperature ^1H NMR study, the most informative region of the spectrum being δ 2.8–2.3 in which the methyl protons are observed. At room temperature, a single broad resonance at δ 2.46 is attributed to the four methyl groups, which upon warming to 60 °C splits into a sharp singlet a δ 2.46 and a broad resonance at δ 2.36 of equal integrated intensities. Further warming results in a gradual sharpening of the up-field signal such that at 110 °C two sharp singlets of approximately equal intensity at δ 2.42 and 2.31 are observed. Comparison with the chemical shift of the methyl substituent in $[\{MoO(S_2CNEt_2)(\mu\text{-}NC_6H_4Me\text{-}o)\}_2]$ **5b** (δ 2.53) leads us to assign tentatively the sharper low-field signal in **6b** to the substituent on the bridging imido ligands. Concomitant with the above are changes in the other regions of the spectrum, most notably the phenyl region transforms from a broad hump into a series of well resolved signals, and the ethyl substituents on the dithiocarbamate ligands sharpen to a well defined quartet and triplet. Cooling the solution below 20 °C leads to further changes in the spectrum such that at −40 °C six sharp resonances are attributed to the methyl substituents which can be separated into three sets with relative intensities 9:2:1 [δ 2.75 (2), 2.70 (9), 2.66 (9), 2.55 (1), 2.46 (1), 2.36 (2)]. We assign these sets of resonances to three rotamers which are present in solution at −40 °C but interconvert at higher temperatures such that at 110 °C interconversion is rapid on the NMR timescale. The fluxional process then involves hindered rotation about the nitrogen–carbon bond of both bridging and terminal imido moieties. This arises due to π conjugation between the metal–nitrogen interaction and the aryl ring (Fig. 6). On the basis of the spectroscopic data it is tempting to suggest that the energy barrier is lower for rotation in the bridging than in the terminal imido functionalities since it is the low-field signal which sharpens at lower temperatures.

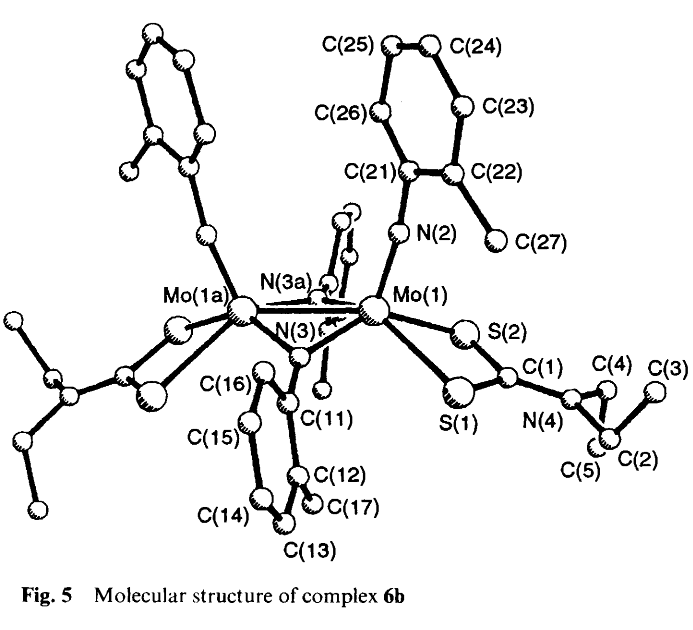

Fig. 5 Molecular structure of complex **6b**

The precise nature of the rotamers observed is difficult to establish. Based on positional isomerism of the methyl groups on the aryl ring and assuming that the ring plane is approximately parallel with the metal–metal vector, there is a total of 16 possible rotamers, 9 of which are unique. The aryl ring could however be frozen out in a position approximately perpendicular to the metal–metal bond as seen in **4b**, thus giving rise to further rotamers. It is tempting to suggest that the major rotamer at low temperature in solution is that preferred in the solid state (Fig. 5). Interestingly in the bis(imido) complex $[\{MoO(S_2CNEt_2)(\mu\text{-}NC_6H_4Me\text{-}o)\}_2]$ **5b** rotamers are not observed in solution or in the solid state. In the latter the methyl groups point in towards the oxo ligands, that is away from the dithiocarbamates, and it appears that this conformation is preferred in the absence of any steric interactions between the relatively bulky *o*-tolyl imido moieties.

Ureato-bridged Complexes $[Mo_2(NPh)_2(S_2CNEt_2)_2(\mu\text{-}X)\{\mu\text{-}PhNC(O)NPh\}]$ **7**.—Thermolysis of a slight excess of phenyl isocyanate with either $[\{MoO(S_2CNEt_2)(\mu\text{-}O)\}_2]$ **2** or $[Mo_2O_2(S_2CNEt_2)_2(\mu\text{-}O)(\mu\text{-}S)]$ **3** leads to the formation of the ureato-bridged complexes $[Mo_2(NPh)_2(S_2CNEt_2)_2(\mu\text{-}NPh)\{\mu\text{-}PhNC(O)NPh\}]$ **7a** and $[Mo_2(NPh)_2(S_2CNEt_2)_2(\mu\text{-}S)\{\mu\text{-}PhNC(O)NPh\}]$ **7b** as red crystalline solids in yields of 90 and 93% respectively [equation (7)]. Characterisation as ureato-bridged complexes was made primarily on the basis of IR spectroscopy, particularly characteristic being the presence of a strong absorption at 1714–1710 cm^{-1} attributed to the C=O moiety of the ureato ligand. In the ^1H NMR spectrum of **7a** the 2.5:1 ratio of phenyl to dithiocarbamate groups further indicated the presence of five NPh moieties, but the complexity of the spectrum did not rule out the possibility of a terminal ureato ligand. In order to confirm the formulation given, an X-ray crystallographic study was carried out on $[Mo_2(NPh)_2(S_2CNEt_2)_2(\mu\text{-}NPh)\{\mu\text{-}PhNC(O)NPh\}]$ **7a** the results of which are summarised in Fig. 7 and Table 5.

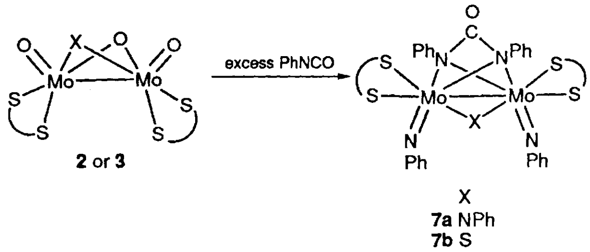

(7)

The structure consists of molybdenum atoms with a highly distorted octahedral co-ordination environment, bridged approximately symmetrically by both imido [Mo(1)–N(3) 1.973(15), Mo(2)–N(3) 1.991(15) Å] and ureato [Mo(1)–N(4) 2.147(13), Mo(2)–N(4) 2.169(13), Mo(1)–N(5) 2.386(14), Mo(2)–N(5) 2.338(14) Å] ligands. The terminal sites are occupied by imido and dithiocarbamate ligands which have the anticipated *cis* geometry. The former are approximately linear

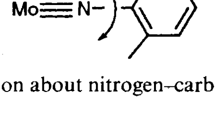

Fig. 6 Restricted rotation about nitrogen–carbon bonds

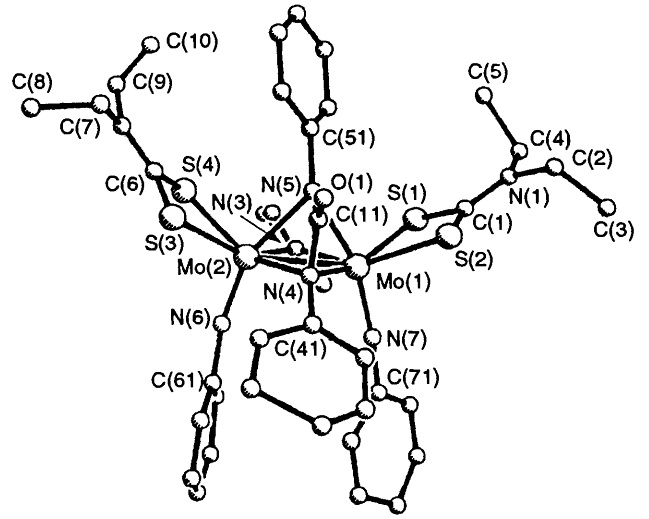

Fig. 7 Molecular structure of complex **7a**

Table 5 Selected bond lengths (Å) and angles (°) for complex **7a**

Mo(1)–Mo(2)	2.625(3)	Mo(1)–S(1)	2.466(6)
Mo(1)–S(2)	2.533(5)	Mo(2)–S(3)	2.546(5)
Mo(2)–S(4)	2.483(6)	Mo(1)–N(3)	1.973(15)
Mo(2)–N(3)	1.991(15)	Mo(1)–N(4)	2.147(13)
Mo(2)–N(4)	2.169(13)	Mo(1)–N(5)	2.386(14)
Mo(2)–N(5)	2.338(14)	Mo(2)–N(6)	1.742(14)
Mo(1)–N(7)	1.740(15)	O(1)–C(11)	1.211(20)
N(4)–C(11)	1.420(20)	N(5)–C(11)	1.386(22)
S(1)–Mo(1)–S(2)	70.6(2)	S(3)–Mo(2)–S(4)	70.2(2)
Mo(1)–N(3)–Mo(2)	82.9(6)	Mo(1)–N(4)–Mo(2)	74.9(4)
Mo(1)–N(5)–Mo(2)	67.5(4)	Mo(2)–N(6)–C(61)	168.4(15)
Mo(1)–N(7)–C(71)	175.1(13)	Mo(1)–Mo(2)–N(6)	105.8(5)
Mo(2)–Mo(1)–N(7)	108.1(5)	N(4)–C(11)–N(5)	101.3(13)

at nitrogen [Mo(1)–N(7)–C(71) 175.1(13), Mo(2)–N(6)–C(61) 168.4(15)°] with the short metal–nitrogen distances [Mo(1)–N(7) 1.740(15), Mo(2)–N(6) 1.742(14)] being similar to those observed in **4a**, **4b** and **6b**. The strong *trans* influence of the terminal imido ligands is clearly seen in the difference in bond lengths to the bridging nitrogens (0.24 Å). Consistent with this is an increase of 7.4° in the angle at N(5) as compared to that at N(4) [Mo(1)–N(5)–Mo(2) 67.5(4), Mo(1)–N(4)–Mo(2) 74.9(4)°]. Both are however considerably closed up with respect to the corresponding angle at the bridging imido ligand [Mo(1)–N(3)–Mo(2) 82.9(6)°]. The dithiocarbamate ligands are also bound quite asymmetrically to the metal centres [Mo(1)–S(1) 2.466(6), Mo(1)–S(2) 2.533(5); Mo(2)–S(3) 2.546(5), Mo(2)–S(4) 2.483(6) Å], those approximately *trans* to the bridging imido moiety being elongated by an average of 0.063 Å. A closer look at the central core geometry is informative. The dihedral angle between the planes containing the dimolybdenum centre and either N(3) or N(4) is 178.5°, while in contrast, a similar plane containing N(5) lies approximately perpendicular to the latter (dihedral angles; 72.0 and 106.5° respectively). The ureato ligand is quite asymmetric as highlighted by the difference of 0.034 Å between the two nitrogen–carbon distances [N(4)–C(11) 1.420(20), N(5)–C(11) 1.386(22) Å]. The carbon–oxygen bond length of 1.211(20) Å is as expected for a ketonic carbonyl, and the bond angle at carbon [N(4)–C(11)–N(5) 101.1(13)°] is similar to those found in related complexes.

The short metal–metal contact of 2.625(3) Å in **7a** is indicative of a direct bonding interaction between the two metal centres and compares well with that of 2.633(1) Å found in the tetraimido complex **6b**. This provides a slight dilemma with regard to electron counting since the molecule is formally a 36-electron complex and thus does not require a metal–metal interaction. This, however, assumes that the three imido ligands act as four-electron donors and the ureato ligand as a six-electron donor. We[12,19] and others[28] have previously shown that even when an imido ligand is linear (terminal) or planar (bridging) it does not necessarily donate its full complement of electrons to a metal centre. In **7a** it may be better to consider the terminal imido ligands as net three-electron donors, with two electrons being in an orbital that is non-bonding with respect to the metal–nitrogen interactions, and we are currently carrying out molecular orbital calculations in order to gain a better insight into the electronic structure.

A handful of bridging ureato complexes have previously been reported,[29,30] the earliest being the diiron complex $[Fe_2(CO)_6\{\mu\text{-}PhNC(O)NPh\}]$ prepared *via* treatment of $[Fe_3(CO)_{12}]$ with phenyl isocyanate.[30] Initial formulation was as the bis(isocyanate) complex $[Fe_2(CO)_6(PhNCO)_2]$, but later its true nature was revealed by an X-ray crystallographic study.[31]

Interconversion of Tetraimido and Ureato-bridged Complexes.—The formation of ureato complexes upon insertion of isocyanates into metal–imido moieties is reasonably well documented.[32] Ureato-bridged complexes **7** can then be envisaged to result from phenyl isocyanate insertion into a bridging imido moiety. In order to investigate this, the tetraimido complex $[\{Mo(NC_6H_4Me\text{-}o)(S_2CNEt_2)(\mu\text{-}NC_6H_4\text{-}Me\text{-}o)\}_2]$ **6b** was heated with an excess of *o*-tolyl isocyanate in order to effect carbon–nitrogen bond formation, however even after prolonged reflux, no reaction was noted.

We have previously postulated that the insertion of an isocyanate into a metal–imido moiety may be reversible.[33] Thus, thermolysis of $[\{Mo(\eta^5\text{-}C_5H_4Me)(NPh)(\mu\text{-}NPh)\}_2]$ with an excess of *p*-tolyl isocyanate resulted in the slow formation of $[\{Mo(\eta^5\text{-}C_5H_4Me)(NC_6H_4Me\text{-}p)(\mu\text{-}NPh)\}_2]$, a consequence of terminal imido exchange, believed to occur *via* reversible formation of a terminal ureato intermediate. In order to investigate this further thermolysis of $[Mo_2(NPh)_2(S_2CNEt_2)_2(\mu\text{-}NPh)\{\mu\text{-}PhNC(O)NPh\}]$ **7a** alone was carried out in toluene. Quite surprisingly, but in accordance with the above experimental observations, cooling of the solution after 18 h led to the deposition of an orange crystalline solid identified as $[\{Mo(NPh)(S_2CNEt_2)(\mu\text{-}NPh)\}_2]$ **6a** in 33% yield. Characterisation proved straightforward by comparison of spectroscopic data with **6b**, most notably the integrated ratio of aryl to dithiocarbamate resonances in the ^1H NMR spectrum was 1 : 1, while in the IR spectrum the strong absorption at 1710 cm^{-1} associated with the ureato ligand was absent. In a further experiment to investigate the mode of formation of the ureato complexes, tetraimido **6a** was heated with 2 equivalents of phenyl isocyanate which resulted in reformation of the ureato-bridged complex **7a** in 72% yield [equation (8)].

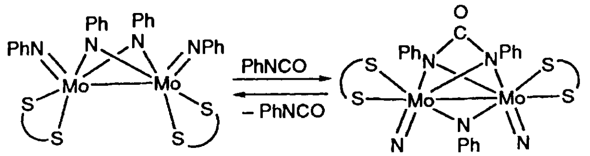

(8)

Hence it appears that ureato-bridged complexes **7a** and **7b** are formed *via* the intermediacy of the imido-bridged complexes **6a** and $[Mo_2(NPh)_2(S_2CNEt_2)_2(\mu\text{-}NPh)(\mu\text{-}S)]$ respectively, by insertion of phenyl isocyanate into a bridging imido moiety. Inspection of the solid-state structures of **6b** and **7a** reveals that isocyanate insertion occurs with relatively little structural reorganisation. Thus if we consider the inserted phenyl isocyanate in **7a** as that defined by C(51)–N(5)–C(11)–O(1), the major structural changes involve a flattening of the Mo_2N_2 core in **6b** by approximately 19°, elongation of the metal–nitrogen distances to the bridging imido ligand by an average of 0.19 Å, and rotation of the phenyl substituent on the attacked imido ligand by approximately 90°. Since reactions of this type are envisaged to proceed *via* nucleophilic attack at the electropositive carbon of the isocyanate, then attack at a bridging rather than a terminal imido ligand suggests that it is the former that is the more nucleophilic. This selectivity is in marked contrast to that observed in the analogous cyclopentadienyl-stabilised system where imido exchange occurs only at the terminal sites.[33]

The difference in reactivity between **6a** and **6b** is difficult to explain in terms of an electronic effect (indeed the substituted imido group should be a better nucleophile), and rather, is believed to be steric in origin. Approach of the isocyanate to either bridging site is blocked by the *o*-methyl substituents while in the ureato-bridged complex it is difficult to arrange all five methyl substituents in a way as to minimise adverse steric interactions between them.

Cationic Bis(imido) Complex $[Mo_2O(S_2CNEt_2)_3(\mu\text{-}NPh)_2][BF_4]$ **8**.—Protonation studies on the related cyclopentadienyl-stabilised mixed oxo–imido complexes have led to an insight into which of the π-donor ligands is the most nucleophilic. For example, protonation of $[Mo_2(\eta^5\text{-}C_5H_4Me)_2O_2(\mu\text{-}O)(\mu\text{-}NPh)]$ has been shown to occur exclusively at a terminal oxo site.[34] In order then to assess which of the π-donor ligands in $[\{MoO(S_2CNEt_2)(\mu\text{-}NPh)\}_2]$ **5a** was the more nucleophilic, protonation of **5a** was carried out. Addition of a slight excess of $HBF_4{\cdot}Et_2O$ to a dichloromethane solution of **5a** resulted in an immediate change from yellow to red and afforded $[Mo_2O(S_2CNEt_2)_3(\mu\text{-}NPh)_2][BF_4]$ **8** as a red crystalline solid in 38% yield [equation (9)]. In the IR spectrum absorptions characteristic of OH or NH units were absent, and while the ^1H NMR spectrum was particularly complex, the most noticeable feature was the 2:3 ratio of aryl to dithiocarbamate resonances. In order to elucidate fully the structure of **8** a crystallographic study was carried out, the results of which are summarised in Fig. 8 and Table 6.

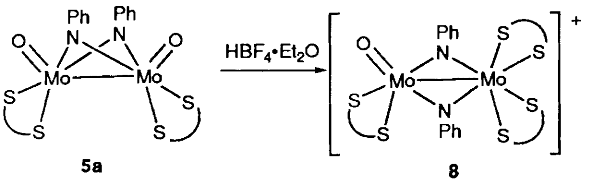

(9)

The molecule consists of two molybdenum atoms in quite different co-ordination environments. Thus, Mo(2) adopts the characteristic square-based pyramidal geometry being bound to a single dithiocarbamate ligand and an oxo moiety [Mo(2)–O(1) 1.650(10) Å], while Mo(1) has a distorted octahedral co-ordination environment being ligated by two dithiocarbamate moieties. The dimolybdenum centre is bridged somewhat asymmetrically by two imido ligands [Mo(1)–N(4) 1.941(9), Mo(2)–N(4) 2.055(15), Mo(1)–N(5) 1.939(15), Mo(2)–N(5) 2.039(9) Å], being on average 0.1 Å closer to Mo(1). The asymmetrical nature of these interactions is easily explained in terms of the positive charge being localised on the octahedral centre, Mo(1). While the molybdenum–molybdenum bond length of 2.654(2) Å is elongated somewhat when compared to that of 2.628(1) Å in the neutral bis(imido) complex $[\{MoO(NC_6H_4Me\text{-}o)(S_2CNEt_2)\}_2]$ **5b**, the major structural difference between the two is the flattening of the central Mo_2N_2 core in the former. Thus in **8**, the dihedral angle between the planes containing both molybdenum atoms and either nitrogen is 175.9° as compared to that of 151.4° in **5b**.

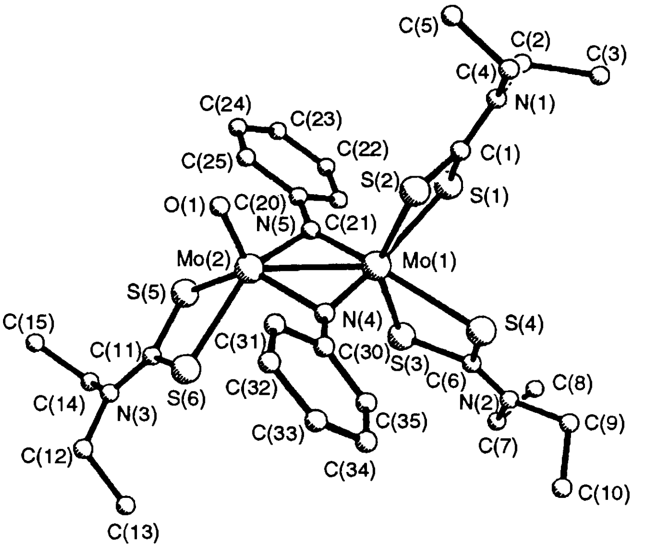

Fig. 8 Molecular structure of complex **8**

Table 6 Selected bond lengths (Å) and angles (°) for complex **8**

Mo(1)–Mo(2)	2.654(2)	Mo(1)–S(1)	2.547(3)
Mo(1)–S(2)	2.451(4)	Mo(1)–S(3)	2.431(4)
Mo(1)–S(4)	2.568(6)	Mo(2)–S(5)	2.455(6)
Mo(2)–S(6)	2.458(4)	Mo(1)–N(4)	1.941(9)
Mo(2)–N(4)	2.055(15)	Mo(1)–N(5)	1.939(15)
Mo(2)–N(5)	2.039(9)	Mo(2)–O(1)	1.650(10)
S(1)–Mo(1)–S(2)	70.5(1)	S(3)–Mo(1)–S(4)	70.2(1)
S(5)–Mo(2)–S(6)	71.5(1)	Mo(1)–N(4)–Mo(2)	83.2(4)
Mo(1)–N(5)–Mo(2)	83.7(4)	O(1)–Mo(2)–O(1)	113.2(4)

As clearly shown by the crystallographic structure, protonation has resulted in substitution of an oxo for a dithiocarbamate ligand. While this appears to be the first example of this type of reaction at a binuclear centre, it is commonplace at mononuclear molybdenum(VI) centres.[35] For example, addition of tetrafluoroboric acid to $[MoO_2(S_2CNEt_2)_2]$ **1** results in the formation of $[MoO(S_2CNEt_2)_3][BF_4]$ in an exactly analogous manner.[27] While we have made no attempt to investigate the mechanism of this reaction, it would seem reasonable to assume that initial protonation occurs at a terminal oxo ligand to afford $[Mo_2O(OH)(\mu\text{-}NPh)_2(S_2CNEt_2)_2]^+$, and the hydroxide produced is displaced by a dithiocarbamate moiety scavenged from a second molecule.

Conclusion

This study has shown that it is possible to prepare dithiocarbamate-stabilised dimeric molybdenum(V) complexes containing imido ligands in either bridging or terminal sites. Their synthesis is relatively straightforward employing oxo substitution by organic isocyanates, and proceeds from both molybdenum(VI) and molybdenum(V) oxide precursors, although higher yields are generally achieved with the latter. The nature of the final product appears to depend critically on the size of the organic substituent at nitrogen. With bulky isocyanates, terminal monosubstitution is noted (albeit in low yield), while with the less sterically hindered aryl isocyanates, multiple substitution reactions occur in good yields, with bridging site substitution occurring initially.

All complexes of the type $[Mo_2X_2(\mu\text{-}X)_2(S_2CNEt)_2]$ exhibit the expected *cis* arrangement of terminally bound ligands and a puckered $Mo_2(\mu\text{-}X)_2$ core as has been found for the related oxo-, sulfido- and seleno-substituted complexes. The bridging imido sites are, however, reactive as exemplified by the insertion of a further unit of isocyanate to afford novel ureato-bridged complexes. While this insertion has previously been noted at mononuclear centres, at the dimolybdenum centre it has been shown to be reversible for the first time.

Experimental

General Procedures.—All reactions were carried out under a nitrogen atmosphere using pre-dried solvents. The NMR spectra were recorded on a Varian VXR 400 spectrometer and IR spectra on a Nicolet 205 FT-IR spectrometer. Column chromatography was carried out on columns of deactivated alumina (6% w/w water). Elemental analysis was performed within the chemistry department of University College. Organic isocyanates were purchased from Aldrich and used as supplied. Dithiocarbamate complexes $[\mathrm{MoO_2(S_2CNEt_2)_2}]$ **1**,[17] $[\{\mathrm{MoO(S_2CNEt_2)_2(\mu\text{-}O)}\}_2]$ **2**[18] and $[\mathrm{Mo_2O_2(S_2CNEt_2)_2(\mu\text{-}O)(\mu\text{-}S)}]$ **3**[18] were prepared by literature methods.

Preparations.—$[\mathrm{Mo_2O(NBu^t)(S_2CNEt_2)_2(\mu\text{-}S)_2}]$ **4a**. Complex **1** (4.01 g, 9.45 mmol) was dissolved in toluene (100 cm^3) and *tert*-butyl isocyanate (1.0 cm^3, 10.1 mmol) was added *via* a degassed syringe. The solution was refluxed for 3 d after which time volatiles were removed at reduced pressure. The resulting solid was absorbed onto alumina and passed down a chromatography column. A red band was obtained after eluting with 40% dichloromethane in light petroleum (b.p. 40–60 °C). Crystals of yellow **4a** (0.60 g, 10%) and red $[\mathrm{Mo(NBu^t)(S_2CNEt_2)_2(\eta^2\text{-}S_2)}]$ (0.90 g, 18%) were obtained upon slow diffusion of methanol into a dichloromethane solution. ^{1}H NMR ($\mathrm{CDCl_3}$): δ 4.00–3.94 (m, 8 H, $\mathrm{CH_2}$), 1.40 (t, 6 H, *J* 7.2, $\mathrm{C}\mathit{H}_3\mathrm{CH_2}$), 1.37, (t, 6 H, *J* 7.1 Hz, $\mathrm{C}\mathit{H}_3\mathrm{CH_2}$), 1.02 [s, 9 H, $\mathrm{C(CH_3)_3}$]. IR $\tilde{\nu}$/cm^{-1}: 1528 (br), 1457m, 1439s, 1379w, 1356m, 1301w, 1281s, 1222s, 1206s, 1154m, 1095w, 1076m, 957s, 848m (Found: C, 26.30; H, 4.40; N, 6.50; S, 29.50. Calc. for $\mathrm{C_{14}H_{29}Mo_2N_3OS_6}$: C, 26.30; H, 4.55; N, 6.55; S, 30.05%).

$[\mathrm{Mo_2O(NC_6H_3Me_2\text{-}2,6)(S_2CNEt_2)_2(\mu\text{-}S)_2}]$ **4b**. Complex **1** (1.34 g, 3.16 mmol) was dissolved in toluene (100 cm^3) and 2,6-dimethylphenyl isocyanate (0.50 cm^3, 3.42 mmol) was added *via* a degassed syringe. The resulting solution was refluxed for 1 d after which the volatiles were removed under reduced pressure. The resulting solid was absorbed onto alumina and passed down a chromatography column. An orange band was obtained upon elution with 25% dichloromethane in light petroleum and shown to be a mixture of $[\mathrm{Mo(NC_6H_3Me\text{-}2,6)(S_2CNEt_2)_2(\eta^2\text{-}S_2)}]$ and **4b** (*ca.* 0.10 g, 4%). A small number of yellow crystals of **4b** were obtained by slow diffusion of methanol into a dichloromethane solution. Satisfactory elemental analysis was not obtained due to persistent contamination of samples with the disulfido complex. ^{1}H NMR ($\mathrm{CDCl_3}$): δ 7.07 (t, 1 H, *J* 7.3, *p*-$\mathrm{C_6H_3}$), 6.96 (d, 2 H, *J* 7.4, *m*-$\mathrm{C_6H_3}$), 4.04–3.65 (m, 8 H, $\mathrm{CH_2}$), 2.51 (s, 6 H, $\mathrm{C}\mathit{H}_3\mathrm{C_6H_3}$), 1.35 (t, 6 H, *J* 7.2, $\mathrm{C}\mathit{H}_3\mathrm{CH_2}$), 1.23 (t, 6 H, *J* 7.2 Hz, $\mathrm{C}\mathit{H}_3\mathrm{CH_2}$). IR $\tilde{\nu}$/cm^{-1}: 1533m, 1516s, 1457m, 1438m, 1378w, 1335m, 1309m, 1278s, 1203m, 1148m, 972m, 764s, 756m, 668m.

$[\mathrm{Mo_2O(NC_{10}H_{15})(S_2CNEt_2)_2(\mu\text{-}S)_2}]$ **4c**. Complex **1** (0.56 g, 1.32 mmol) and adamantyl isocyanate ($\mathrm{C_{10}H_{15}NC}$) (0.22 g, 1.33 mmol) were dissolved in toluene (100 cm^3). The resulting solution was refluxed for 3 d after which volatiles were removed under reduced pressure. The resulting solid was absorbed onto alumina and passed down a chromatography column. A red band was obtained after eluting with 40% dichloromethane in light petroleum. Crystals of yellow **4c** (0.15 g, 32%) and red $[\mathrm{Mo(NC_{10}H_{15})(S_2CNEt_2)_2(\eta^2\text{-}S_2)}]$ (0.24 g, 31%) were obtained by slow diffusion of methanol into a dichloromethane solution. ^{1}H NMR ($\mathrm{CDCl_3}$): δ 4.06–3.86 (m, 8 H, $\mathrm{CH_2}$), 1.87 (br s, 3 H, $\mathrm{C_{10}H_{15}}$), 1.61 (br s, 6 H, $\mathrm{C_{10}H_{15}}$), 1.56 (s, 6 H, $\mathrm{C_{10}H_{15}}$), 1.40 (t, 6 H, *J* 7.2, $\mathrm{CH_3}$), 1.36 (t, 6 H, *J* 7.2 Hz, $\mathrm{CH_3}$). IR $\tilde{\nu}$/cm^{-1}: 1531s, 1502s, 1452m, 1438m, 1357m, 1298w, 1280s, 1229m, 1204m, 1148w, 1095w, 1087w, 1075w, 953s, 845w, 482w (Found: C, 32.90; H, 4.80; N, 5.75; S, 26.75. Calc. for $\mathrm{C_{20}H_{35}Mo_2N_4OS_6}$: C, 33.45; H, 4.90; N, 5.85; S, 26.80%).

$[\{\mathrm{MoO(S_2CNEt_2)_2(\mu\text{-}NPh)}\}_2]$ **5a**. Complex **1** (1.13 g, 2.66 mmol) was dissolved in toluene (100 cm^3) and phenyl isocyanate (0.25 cm^3, 2.66 mmol) was added *via* a degassed syringe. The solution was refluxed for 3 d after which volatiles were removed under reduced pressure. The resulting solid was absorbed onto alumina and passed down a chromatography column. A yellow band, identified as $\mathrm{(Et_2NCS)_2S_2}$ by comparison of its IR spectrum with that of an authentic sample, was obtained after elution with 20% dichloromethane in light petroleum. Elution with 90% dichloromethane in light petroleum gave yellow $[\{\mathrm{MoO(S_2CNEt_2)_2(\mu\text{-}NPh)}\}_2]$ **5a** (0.74 g, 76%). Crystals were obtained by slow diffusion of methanol into a dichloromethane solution. ^{1}H NMR ($\mathrm{CDCl_3}$): δ 7.43 (t, 4 H, *J* 7.1, *m*-$\mathrm{C_6H_5}$), 7.31 (d, 4 H, *J* 7.0, *o*-$\mathrm{C_6H_5}$), 7.17 (t, 2 H, *J* 7.1, *p*-$\mathrm{C_6H_5}$), 3.86 (q, 8 H, *J* 7.0, $\mathrm{CH_2}$), 1.30 (t, 12 H, *J* 7.0 Hz, Me). IR $\tilde{\nu}$/cm^{-1}: 1585m, 1524vs, 1476s, 1457s, 1439s, 1381w, 1356w, 1278s, 1202m, 1151m, 1075m, 948s, 932s, 768m, 695m (Found: C, 37.65; H, 4.25; N, 7.85; S, 17.50. Calc. for $\mathrm{C_{22}H_{30}Mo_2N_4O_2S_4}$: C, 37.60; H, 4.30; N, 7.80; S, 18.25%).

$[\{\mathrm{MoO(\mu\text{-}NC_6H_4Me\text{-}\mathit{o})(S_2CNEt_2)}\}_2]$ **5b**. To a dichloromethane (20 cm^3) solution of complex **6b** (0.30 g, 0.33 mmol) was added a few drops of aqueous trifluoroacetic acid. An initial change from orange to red was observed, gradually becoming yellow over a minute. The solvent was removed on a rotary evaporator, and the resulting oily yellow solid washed with diethyl ether. Crystals of **5b** (0.20 g, 83%) were obtained by slow diffusion of methanol into a dichloromethane solution. ^{1}H NMR ($\mathrm{CDCl_3}$): δ 7.38 (d, 2 H, *J* 7.1, $\mathrm{C_6H_4}$), 7.15–7.10 (m, 4 H, $\mathrm{C_6H_4}$), 6.50 (d, 2 H, *J* 7.1, $\mathrm{C_6H_4}$), 3.86–3.78 (m, 8 H, $\mathrm{CH_2}$), 2.53 (s, 6 H, $\mathrm{C_6H_4C}\mathit{H}_3$), 1.27 (t, 12 H, *J* 7.0 Hz, $\mathrm{CH_2C}\mathit{H}_3$). IR $\tilde{\nu}$/cm^{-1}: 1580m, 1520s, 1481s, 1456s, 1439s, 1380w, 1351w, 1279s, 1201m, 1151m, 1076m, 948s, 932s, 756m, 718m (Found: C, 39.00; H, 4.40; N, 8.30; S, 18.40. Calc. for $\mathrm{C_{24}H_{34}Mo_2N_4O_2S_4}$: C, 39.45; H, 4.70; N, 7.65; S, 17.55%).

$[\{\mathrm{MoO(\mu\text{-}NC_6H_4Me\text{-}\mathit{p})(S_2CNEt_2)}\}_2]$ **5c**. Complex **1** (0.58 g, 1.36 mmol) was dissolved in toluene (100 cm^3) and *p*-tolyl isocyanate (0.19 cm^3, 1.42 mmol) was added *via* a degassed syringe. The resulting solution was refluxed for 3 d after which volatiles were removed under reduced pressure. The resulting solid was absorbed onto alumina and passed down a chromatography column. Elution with 5% methanol in dichloromethane gave yellow **5c** (0.50 g, 50%). Crystals were obtained by slow diffusion of methanol into a dichloromethane solution. ^{1}H NMR ($\mathrm{CDCl_3}$): δ 7.37 (s, 4 H, $\mathrm{C_6H_4}$), 3.86 (q, 8 H, *J* 7.3, $\mathrm{CH_2}$), 2.43 (s, 6 H, $\mathrm{C_6H_4C}\mathit{H}_3$), 1.30 (t, 12 H, *J* 7.3 Hz, $\mathrm{CH_2C}\mathit{H}_3$). IR $\tilde{\nu}$/cm^{-1}: 1522s, 1497s, 1458m, 1440m, 1380w, 1357w, 1277s, 1203m, 1151w, 1096w, 1077w, 946s, 930m, 826m (Found: C, 39.85; H, 4.45; N, 7.55; S, 17.00. Calc. for $\mathrm{C_{24}H_{34}Mo_2N_4O_2S_4}$: C, 39.45; H, 4.70; N, 7.65; S, 17.55%).

$[\{\mathrm{Mo(NPh)(S_2CNEt_2)(\mu\text{-}NPh)}\}_2]$ **6a**. Complex **7a** (1.20 g, 1.23 mmol) was dissolved in toluene (100 cm^3) and refluxed for 18 h. Upon cooling orange crystals were deposited. These were isolated by filtration of the solution, followed by washing with light petroleum (2 × 50 cm^3) and identified as **6a** (0.35 g, 33%). ^{1}H NMR ($\mathrm{CDCl_3}$): δ 8.12 (d, 4 H, *J* 7.3), 7.52 (t, 4 H, *J* 7.4), 7.20 (t, 2 H, *J* 7.2), 7.13 (t, 4 H, *J* 7.4), 6.74 (t, 2 H, *J* 7.4), 6.67 (d, 4 H, *J* 7.4), 3.68 (q, 8 H, *J* 7.3, $\mathrm{CH_2}$), 1.18 (t, 12 H, *J* 7.2 Hz, $\mathrm{CH_3}$). IR $\tilde{\nu}$/cm^{-1}: 1578m, 1516s, 1474s, 1436m, 1354w, 1309m, 1274m, 1262m, 1201w, 1149m, 1067m, 1023w, 996w, 975w, 767s, 754s, 695m, 686m, 668m, 486w (Found: C, 47.65; H, 4.70; N, 9.55; S, 15.10. Calc. for $\mathrm{C_{34}H_{40}Mo_2N_6S_4}$: C, 47.90; H, 4.70; N, 9.85; S, 15.10%).

$[\{\mathrm{Mo(NC_6H_4Me\text{-}\mathit{o})(S_2CNEt_2)(\mu\text{-}NC_6H_4Me\text{-}\mathit{o})}\}_2]$ **6b**. *Method* (*i*). Complex **1** (1.02 g, 2.40 mmol) was dissolved in toluene (100 cm^3) and *o*-tolyl isocyanate (0.32 cm^3, 2.41 mmol) was added *via* a degassed syringe. The resulting solution was refluxed for 3 d after which volatiles were removed under reduced pressure. The resulting solid was absorbed onto alumina and passed down a chromatography column. Elution

Table 7 Crystallographic data

	4a	**4b**	**5b**	**6b**	**7a**·MeOH	**8**
Formula	$C_{14}H_{29}Mo_2N_3OS_6$	$C_{18}H_{29}Mo_2N_3OS_6$	$C_{24}H_{34}Mo_2N_4O_2S_4$	$C_{38}H_{48}Mo_2N_6S_4$	$C_{42}H_{49}Mo_2N_7O_2S_4$	$C_{27}H_{40}BF_4Mo_2N_5S_6O$
M	639.70	758.80	730.74	909.04	1004.10	923.79
Crystal system	Monoclinic	Monoclinic	Monoclinic	Monoclinic	Orthorhombic	Triclinic
Space group	$P2_1/a$	$C2/c$	$P2_1/c$	$C2/c$	$P2_12_12_1$	$P\bar{1}$
a/Å	12.7113(19)	15.9806(18)	9.9634(23)	20.6392(30)	11.8520(53)	11.0575(33)
b/Å	11.8815(30)	13.8062(30)	13.7055(16)	10.8102(10)	17.7818(73)	14.7731(42)
c/Å	17.1932(33)	24.8973(34)	22.2125(42)	20.4253(29)	22.5184(64)	14.8527(41)
α/°	90	90	90	90	90	63.240(21)
β/°	96.908(14)	95.530(10)	97.853(17)	113.210(11)	90	69.270(24)
γ/°	90	90	90	90	90	69.930(23)
U/Å^3	2578.37	5466.63	3004.76	4188.15	4745.75	1976.46
Z	4	8	4	4	4	2
$F(000)$	1288	2768	1480	1864	2056	936
D_c/g cm^{-3}	1.65	1.67	1.61	1.44	1.40	1.55
Crystal size/mm	0.50 × 0.30 × 0.22	0.70 × 0.40 × 0.40	0.55 × 0.35 × 0.25	0.80 × 0.40 × 0.40	0.52 × 0.42 × 0.30	0.52 × 0.26 × 0.16
μ(Mo-Kα)/cm^{-1}	14.27	13.53	11.10	8.09	9.10	9.70
Orientation reflections: no, 2θ range/°	30, 27–22	30, 21–31	30, 21–30	29, 15–32	30, 16–25	24, 10–22
Data measured	5054	6348	5899	5871	4816	7390
Unique data	5022	6318	5845	5754	3317	7161
No. of unique with $I \geqslant 3.0\sigma(I)$	3963	4065	4580	3179	2757	3569
No. of parameters	235	271	325	246	267	415
R^a	0.034	0.032	0.032	0.035	0.076	0.068
R'^b	0.038	0.034	0.041	0.039	0.081	0.071
Largest shift/e.s.d., final cycle	0.001	0.001	0.001	0.004	0.009	0.003
Largest peak/e Å^{-3}	1.24	0.36	0.36	0.61	0.93	1.07

[a] $R = \Sigma(|F_o| - |F_c|)/\Sigma|F_o|$. [b] $R' = \Sigma w^{\frac{1}{2}}(|F_o| - |F_c|)/\Sigma w^{\frac{1}{2}}|F_o|$.

Table 8 Atomic coordinates (× 10^4) for complex **4a**

Atom	*x*	*y*	*z*
Mo(1)	1 955(1)	2 045(1)	7 843(1)
Mo(2)	1 822(1)	30(1)	6 968(1)
S(1)	854(2)	2 939(1)	8 774(1)
S(2)	3 070(2)	2 445(1)	9 089(1)
S(3)	2 873(1)	−1 744(1)	7 064(1)
S(4)	612(2)	−1 632(1)	6 929(1)
S(5)	439(1)	995(1)	7 456(1)
S(6)	3 310(1)	754(1)	7 722(1)
N(1)	2 021(4)	3 588(4)	10 100(2)
N(2)	1 683(4)	−3 592(3)	7 191(2)
N(3)	1 851(4)	519(3)	6 039(2)
O(1)	2 069(4)	3 083(3)	7 204(2)
C(1)	1 992(5)	3 075(4)	9 423(3)
C(2)	3 015(6)	3 653(6)	10 650(3)
C(3)	3 698(7)	4 614(7)	10 472(4)
C(4)	1 084(5)	4 136(5)	10 345(3)
C(5)	474(6)	3 397(6)	10 824(4)
C(6)	1 723(5)	−2 495(4)	7 065(3)
C(7)	2 655(5)	−4 242(4)	7 397(3)
C(8)	2 904(6)	−4 405(6)	8 270(4)
C(9)	680(5)	−4 200(4)	7 165(3)
C(10)	324(6)	−4 684(6)	6 362(4)
C(11)	1 871(7)	1 159(5)	5 320(3)
C(12)	1 728(9)	325(7)	4 639(4)
C(13)	2 918(8)	1 746(7)	5 353(5)
C(14)	1 001(8)	2 014(6)	5 257(4)

Table 9 Atomic coordinates (× 10^4) for complex **4b**

Atom	*x*	*y*	*z*
Mo(1)	6 082(1)	1 495(1)	6 714(1)
Mo(2)	7 656(1)	1 755(1)	6 323(1)
S(1)	4 804(1)	2 497(1)	6 654(1)
S(2)	4 860(1)	489(1)	6 402(1)
S(3)	8 402(1)	1 007(1)	5 600(1)
S(4)	8 308(1)	3 026(1)	5 803(1)
S(5)	6 708(1)	2 951(1)	6 503(1)
S(6)	6 796(1)	400(1)	6 218(1)
N(1)	3 398(2)	1 437(3)	6 453(2)
N(2)	9 283(3)	2 308(3)	5 083(2)
N(3)	8 323(2)	1 642(3)	6 901(1)
O(1)	6 315(2)	1 238(3)	7 364(1)
C(1)	4 222(3)	1 465(3)	6 503(2)
C(2)	2 910(3)	2 302(4)	6 545(3)
C(3)	2 727(5)	2 913(5)	6 070(3)
C(4)	2 933(3)	535(4)	6 340(2)
C(5)	2 488(5)	463(5)	5 806(3)
C(6)	8 749(3)	2 129(4)	5 443(2)
C(7)	9 556(4)	3 294(5)	4 967(3)
C(8)	10 307(5)	3 633(5)	5 291(3)
C(9)	9 623(4)	1 545(5)	4 767(2)
C(10)	10 472(5)	1 252(6)	4 968(3)
C(11)	8 738(2)	1 588(3)	7 419(2)
C(12)	8 974(3)	2 459(5)	7 692(2)
C(13)	9 397(3)	2 374(6)	8 195(2)
C(14)	9 574(4)	1 490(7)	8 426(2)
C(15)	9 341(3)	645(6)	8 163(2)
C(16)	8 914(3)	675(4)	7 644(2)
C(17)	8 773(4)	3 427(4)	7 436(3)
C(18)	8 655(4)	−217(4)	7 340(2)

with 25% dichloromethane in light petroleum afforded orange **6b** (0.38 g, 34%). Crystals were obtained by slow diffusion of methanol into a dichloromethane solution. ^{1}H NMR ([^{2}H$_8$]toluene) (383 K): δ 7.25 (br, 2 H, Ph), 7.20 (d, 2 H, *J* 7.2, Ph), 7.15 (t, 2 H, *J* 7.5, Ph), 6.92 (d, 2 H, *J* 8.3, Ph), 6.88 (d, 2 H, *J* 8.8, Ph), 6.75 (d, 2 H, *J* 6.7, Ph), 6.57 (m, 4 H, Ph), 3.28 (q, 8 H, *J* 7.0, CH$_2$), 2.42 (s, 6 H, CH$_3$), 2.31 (s, 6 H, CH$_3$), 0.75 (t, 12 H, *J* 7.0, CH$_2$C*H*$_3$); (233 K) δ 8.15–6.65 (m, Ph), 2.98 (m, CH$_2$), 2.75 (s, CH$_3$), 2.70 (s, CH$_3$), 2.66 (s, CH$_3$), 2.55 (s, CH$_3$), 2.46 (s, CH$_3$), 2.36 (s, CH$_3$), 0.62 (t, *J* 6.8, CH$_2$C*H*$_3$), 0.56 (t, *J* 7.0, CH$_2$C*H*$_3$). IR ν/cm^{-1}: 1515s, 1472m, 1455m, 1437m, 1321m, 1272s, 1263s, 1204w, 1150w, 1113w, 1076w, 992w, 756s, 718w (Found: C, 49.75; H, 5.25; N, 9.10; S, 14.20. Calc. for $C_{38}H_{48}Mo_2N_6S_4$: C, 50.20; H, 5.30; N, 9.10; S, 14.10%).

Method (*ii*). To a toluene (100 cm^3) solution of complex **2** (0.21 g, 0.38 mmol) was added phenyl isocyanate (0.2 cm^3, 1.88 mmol). The resulting solution was refluxed for 16 h during which time it changed from yellow to orange. Solvents were removed under reduced pressure and the resultant orange solid absorbed onto alumina and passed down a chromatography column. Elution with 40% dichloromethane in light petroleum gave an orange band identified as **6b** (0.31 g, 90%).

[Mo$_2$(NPh)$_2$(S$_2$CNEt$_2$)$_2$(μ-NPh){μ-PhNC(O)NPh}] **7a**. *Method* (*i*). To a toluene (100 cm^3) solution of [{MoO(μ-O)(S$_2$CNEt$_2$)}$_2$] **2** (0.12 g, 0.22 mmol) was added phenyl isocyanate (0.13 cm^3, 1.10 mmol). The resulting solution was refluxed for 16 h during which it changed from yellow to red. Solvents were removed at reduced pressure and the resultant red solid absorbed onto alumina and passed down a chromatography column. Elution with dichloromethane gave a red band identified as **7a** (0.31 g, 90%). ^{1}H NMR (CDCl$_3$): δ 7.88 (d, 2 H, *J* 7.2), 7.41 (d, 2 H, *J* 7.4), 7.30 (t, 4 H, *J* 7.2), 7.15 (t, 2 H, *J* 7.3), 7.08 (d, 2 H, *J* 7.4), 6.96 (t, 2 H, *J* 7.4), 6.86 (t, 2 H, *J* 7.3), 6.81–6.73 (m, 4 H), 6.66 (t, 1 H, *J* 7.3), 6.38 (d, 4 H, *J* 7.3), 3.84 (m, 4 H, CH$_2$), 3.65 (sxt, 2 H, *J* 7.2, CH$_2$), 3.52 (sxt, 2 H, *J* 7.1, CH$_2$), 1.20 (t, 6 H, *J* 7.2, Me), 0.98 (t, 6 H, *J* 7.2, CH$_3$). IR $\tilde{\nu}$/cm^{-1}: 1710s, 1696s, 1583m, 1580m, 1512vs, 1474s, 1439s, 1355m, 1318s, 1274s, 1252s, 1205m, 1149m, 1072m, 1023m, 754s, 687s (Found: C, 49.95; H, 4.60; N, 9.70; S, 13.15. Calc. for $C_{41}H_{45}Mo_2N_7OS_4$: C, 50.65; H, 4.65; N, 10.10; S, 13.20%).

Method (*ii*). To a solution of complex **6a** (0.34 g, 0.40 mmol) in toluene (100 cm^3) was added phenyl isocyanate (1.00 cm^3, 0.90 mmol). The resulting mixture was refluxed for 3 d after which volatiles were removed at reduced pressure, and the products purified by chromatography. Elution with dichloromethane gave a red band, **7a** (0.28 g, 72%).

Method (*iii*). Complex **1** (2.44 g, 5.75 mmol) was dissolved in toluene (100 cm^3) and to this was added phenyl isocyanate (1.40 cm^3, 11.7 mmol). The resulting solution was refluxed for 3 d, after which volatiles were removed under reduced pressure. The remaining red solid was passed down a chromatography column. Elution with 90% dichloromethane in light petroleum gave **7a** (1.45 g, 52%).

[Mo$_2$(NPh)$_2$(S$_2$CNEt$_2$)$_2$(μ-S){μ-PhNC(O)NPh}] **7b**. To a toluene (100 cm^3) solution of complex **3** (0.22 g, 0.39 mmol), phenyl isocyanate (0.19 cm^3, 1.60 mmol) was added *via* a degassed syringe. The resulting solution was refluxed for 16 h during which it changed from yellow to red. Solvents were removed at reduced pressure and the resultant red solid absorbed onto alumina and passed down a chromatography column. Elution with 60% dichloromethane in light petroleum gave a red band identified as **7b** (0.33 g, 93%). ^{1}H NMR (CDCl$_3$): δ 7.88 (d, 2 H, *J* 7.3, *o*-C$_6$H$_5$), 7.25 (t, 2 H, *J* 6.8, *p*-C$_6$H$_5$), 7.20 (t, 1 H, *J* 7.1, *p*-C$_6$H$_5$), 7.04 (d, 2 H, *J* 7.3, *o*-C$_6$H$_5$), 6.89 (t, 4 H, *J* 7.8, *m*-C$_6$H$_5$), 6.79 (t, 4 H, *J* 7.3, *m*-C$_6$H$_5$), 6.71 (t, 1 H, *J* 7.3, *p*-C$_6$H$_5$), 6.56 (d, 4 H, *J* 8.0, *o*-C$_6$H$_5$), 4.00–3.94 (m, 4 H, CH$_2$), 3.66 (sxt, 2 H, *J* 7.2, CH$_2$), 3.57 (sxt, 2 H, *J* 7.2, CH$_2$) 1.29 (t, 6 H, *J* 7.2, CH$_3$), 1.05 (t, 6 H, *J* 7.2 Hz, CH$_3$). IR $\tilde{\nu}$/cm^{-1}: 1714s, 1521s, 1486s, 1474s, 1450m, 1438m, 1312s, 1277s, 1247m, 759m, 689m (Found: C, 44.90; H, 4.35; N, 8.80; S, 17.15. Calc. for $C_{35}H_{40}Mo_2N_6OS_5{\cdot}0.5CH_2Cl_2$: C, 44.65; H, 4.30; N, 8.80; S, 16.75%).

[Mo$_2$O(S$_2$CNEt$_2$)$_3$(μ-NPh)$_2$][BF$_4$] **8**. To a dichloromethane (30 cm^3) solution of [{MoO(S$_2$CNEt$_2$)(μ-NPh)}$_2$] **5a** (0.20 g, 0.28 mmol) was added a 0.01 cm^3 of an ethereal solution of HBF$_4$ (85%). The solution rapidly turned from yellow to red. The solvent was removed and the remaining red oil was washed with diethyl ether. The compound was dissolved in dichloromethane and a few drops of hexane were added. Upon refrigeration red crystals of **8** (0.10 g, 38%) were formed. ^{1}H NMR (CDCl$_3$): δ 7.49 (t, 4 H, *J* 7.1, *m*-C_6H_5), 7.29 (d, 4 H, *J* 7.0, *o*-C_6H_5), 7.10 (t, 2 H, *J* 7.1 Hz, *p*-C_6H_5), 3.70–4.01 (m, 12 H, CH_2), 1.00–1.31 (m, 18 H, CH_3). IR $\tilde{\nu}$/cm^{-1}: 1526m, 1442m, 1382w, 1355w, 1280m, 1200w, 1154w, 1052s (br), 996w, 964w, 847w, 788w, 691w, 520w (Found: C, 36.25; H, 4.25; N, 7.65; S,

Table 10 Atomic coordinates (× 10^4) for complex **5b**

Atom	*x*	*y*	*z*
Mo(1)	2842(1)	7742(1)	4019(1)
Mo(2)	1787(1)	7596(1)	2872(1)
S(1)	5177(1)	7713(1)	4590(1)
S(2)	2919(1)	6562(1)	4858(1)
S(3)	2953(1)	7228(1)	1990(1)
S(4)	486(1)	6325(1)	2242(1)
N(1)	5206(3)	6715(3)	5643(1)
N(2)	1557(4)	5951(3)	1226(1)
N(3)	3605(3)	8000(2)	3266(1)
N(4)	1408(3)	6895(3)	3599(1)
O(1)	2151(3)	8763(2)	4271(1)
O(2)	786(3)	8589(2)	2738(1)
C(1)	4538(4)	6962(3)	5107(2)
C(2)	6589(5)	7062(4)	5853(2)
C(3)	6568(6)	7929(6)	6276(3)
C(4)	4604(5)	6079(3)	6059(2)
C(5)	4884(6)	5015(4)	5964(2)
C(6)	1643(4)	6433(3)	1736(2)
C(7)	2538(5)	6084(4)	789(2)
C(8)	3424(6)	5198(5)	748(3)
C(9)	380(5)	5316(3)	1025(2)
C(10)	−669(6)	5846(4)	599(3)
C(11)	4835(4)	8274(3)	3067(2)
C(12)	4949(5)	9188(3)	2802(2)
C(13)	6217(5)	9427(4)	2621(2)
C(14)	7298(5)	8797(4)	2693(2)
C(15)	7152(5)	7902(5)	2943(2)
C(16)	5929(4)	7642(3)	3128(2)
C(17)	3788(6)	9885(3)	2730(3)
C(21)	651(4)	6088(3)	3764(2)
C(22)	−353(4)	6198(4)	4140(2)
C(23)	−1012(5)	5345(5)	4295(2)
C(24)	−739(5)	4447(5)	4071(3)
C(25)	229(5)	4349(4)	3693(2)
C(26)	919(4)	5168(3)	3550(2)
C(27)	−677(6)	7181(5)	4384(3)

Table 11 Atomic coordinates (× 10^4) for complex **6b**

Atom	*x*	*y*	*z*
Mo(1)	664(1)	2328(1)	2951(1)
S(1)	1742(1)	3344(1)	2951(1)
S(2)	1273(1)	3445(1)	4100(1)
N(1)	2571(2)	4142(3)	4244(2)
N(2)	946(2)	803(3)	3144(2)
N(3)	224(2)	2657(3)	1926(2)
C(1)	1955(2)	3697(3)	3830(2)
C(2)	3133(2)	4328(5)	3980(3)
C(4)	2731(3)	4516(5)	4984(2)
C(3)	3598(3)	3218(7)	4093(4)
C(5)	2593(3)	5886(6)	5024(3)
C(11)	423(2)	2918(4)	1356(2)
C(12)	571(3)	4107(6)	1211(3)
C(13)	754(4)	4310(9)	631(5)
C(14)	797(4)	3401(13)	227(5)
C(15)	634(3)	2208(10)	338(3)
C(16)	447(3)	1938(7)	910(3)
C(17)	514(5)	5089(8)	1568(6)
C(17A)	254(7)	872(12)	980(7)
C(21)	1120(3)	−430(4)	3144(2)
C(22)	1753(4)	−737(5)	3024(3)
C(23)	1898(5)	−1987(8)	3030(4)
C(24)	1487(6)	−2838(7)	3131(4)
C(25)	925(6)	−2612(7)	3265(4)
C(26)	724(4)	−1324(6)	3269(3)
C(27)	2225(5)	182(9)	2990(6)
C(27A)	269(8)	−1163(13)	3483(8)

Table 12 Atomic coordinates (× 10^4) for complex **7a**

Atom	*x*	*y*	*z*
Mo(1)	1788(1)	4340(1)	956(1)
Mo(2)	1471(1)	5674(1)	1428(1)
S(1)	372(5)	3411(3)	631(2)
S(2)	2348(5)	3820(3)	−49(2)
S(3)	1723(5)	7036(3)	1106(2)
S(4)	−329(5)	6369(3)	1558(2)
O(1)	2730(11)	5872(7)	−121(5)
N(1)	707(15)	2920(9)	−471(7)
N(2)	−280(15)	7676(9)	988(7)
N(3)	591(13)	4722(8)	1485(6)
N(4)	2810(12)	5325(7)	832(6)
N(5)	1159(13)	5420(8)	422(6)
N(6)	2258(12)	5682(9)	2081(6)
N(7)	2643(13)	3824(9)	1434(7)
C(1)	1094(18)	3296(11)	−21(9)
C(2)	1429(25)	2832(15)	−1053(11)
C(3)	2187(34)	2176(21)	−1063(16)
C(4)	−392(25)	2563(15)	−444(12)
C(5)	−1270(22)	3022(14)	−641(11)
C(6)	305(18)	7140(11)	1187(8)
C(7)	236(24)	8298(13)	609(11)
C(8)	262(27)	9050(16)	935(13)
C(9)	−1554(22)	7698(15)	1015(10)
C(10)	−2153(41)	7270(26)	561(19)
C(11)	2284(14)	5566(9)	298(7)
C(31)	−214(16)	4374(11)	1852(8)
C(32)	0(25)	3682(15)	2124(11)
C(33)	−809(21)	3312(14)	2467(10)
C(34)	−1803(24)	3651(15)	2528(11)
C(35)	−2090(28)	4292(20)	2294(13)
C(36)	−1273(24)	4688(16)	1908(12)
C(41)	4049(16)	5426(10)	884(8)
C(42)	4463(24)	6102(15)	1035(10)
C(43)	5700(31)	6258(21)	1087(14)
C(44)	6358(30)	5586(19)	949(12)
C(45)	5981(33)	4981(21)	809(15)
C(46)	4753(29)	4868(18)	743(13)
C(51)	272(14)	5630(10)	15(7)
C(52)	−684(16)	5238(11)	4(8)
C(53)	−1620(22)	5433(13)	−328(9)
C(54)	−1534(22)	6089(13)	−673(10)
C(55)	−565(23)	6491(15)	−638(11)
C(56)	314(18)	6327(11)	−297(8)
C(61)	2903(17)	5536(11)	2570(8)
C(62)	4015(21)	5771(15)	2595(11)
C(63)	4664(23)	5606(15)	3109(10)
C(64)	4242(21)	5139(12)	3550(11)
C(65)	3208(23)	4918(14)	3516(11)
C(66)	2500(22)	5055(13)	3026(9)
C(71)	3342(16)	3456(10)	1857(7)
C(72)	4319(20)	3839(14)	2084(10)
C(73)	4935(25)	3491(15)	2496(13)
C(74)	4643(28)	2799(17)	2689(12)
C(75)	3694(26)	2431(17)	2452(13)
C(76)	3061(22)	2774(13)	2003(10)
O(90)	1728(29)	845(19)	1635(14)
O(91)	783(30)	1122(18)	617(15)
C(90)	681(54)	917(33)	1836(26)
C(91)	−415(43)	1186(26)	1103(19)

Table 13 Atomic coordinates (× 10^4) for complex **8**

Atom	*x*	*y*	*z*	Atom	*x*	*y*	*z*
Mo(1)	4056(1)	2846(1)	3409(1)	C(10)	5429(19)	1609(13)	−200(12)
Mo(2)	4614(1)	4429(1)	3462(1)	C(11)	6995(15)	5315(11)	2514(13)
S(1)	3376(3)	1202(3)	4854(3)	C(12)	8161(18)	6661(13)	1068(15)
S(2)	1634(3)	3166(3)	3999(3)	C(13)	8783(22)	6367(17)	169(18)
S(3)	6124(3)	1806(3)	2749(3)	C(14)	9149(18)	5367(14)	2596(16)
S(4)	3707(3)	2252(3)	2155(3)	C(15)	8947(18)	5909(16)	3274(17)
S(5)	6782(4)	4290(3)	3675(3)	C(20)	5351(13)	2291(10)	5253(10)
S(6)	5693(4)	5730(3)	1920(3)	C(21)	5961(13)	1236(10)	5482(11)
N(1)	705(12)	1487(9)	5526(9)	C(22)	6414(14)	691(10)	6372(10)
N(2)	5933(11)	1007(8)	1508(8)	C(23)	6271(14)	1132(12)	7060(12)
N(5)	4846(10)	2884(8)	4364(8)	C(24)	5654(16)	2154(13)	6838(11)
N(4)	3883(10)	4284(7)	2451(8)	C(25)	5177(14)	2747(11)	5957(12)
N(3)	8006(13)	5783(9)	2075(11)	C(30)	3271(12)	5060(10)	1688(11)
O(1)	3392(10)	5015(7)	4181(8)	C(31)	2548(13)	6012(11)	1778(12)
C(1)	1765(12)	1868(11)	4871(11)	C(32)	1953(14)	6818(12)	999(14)
C(2)	849(14)	444(10)	6349(11)	C(33)	2072(16)	6704(14)	111(14)
C(3)	630(16)	−378(12)	6111(14)	C(34)	2814(18)	5753(14)	−1(13)
C(4)	−644(13)	2104(12)	5505(14)	C(35)	3406(17)	4938(12)	774(13)
C(5)	−1107(17)	2680(16)	6222(18)	B(1)	1300(26)	638(21)	900(26)
C(6)	5342(13)	1599(9)	2028(10)	F(1)	1303(13)	−369(9)	1280(10)
C(7)	7360(13)	444(11)	1427(12)	F(2)	2476(14)	842(11)	244(13)
C(8)	7483(17)	−722(11)	2116(13)	F(3)	434(21)	1220(13)	443(30)
C(9)	5223(16)	879(12)	893(10)	F(4)	1230(36)	943(18)	1593(16)

21.10. Calc. for $C_{29}H_{40}BF_4Mo_2N_5OS_6$: C, 36.85; H, 4.25; N, 7.40; S, 20.30%).

Crystal Structure Determinations.—Details of the crystal structure analyses of complexes **6b**[22] and **7a**[21] have been given in earlier communications. Crystals were mounted on a glass fibre. All geometric and intensity data were taken from this sample using an automated four-circle diffractometer (Nicolet R3mV) equipped with Mo-Kα radiation (λ = 0.710 73 Å) at 19 ± 1 °C. The lattice vectors were identified by application of the automatic indexing routine of the diffractometer to the positions of a number of reflections taken from a rotation photograph and centred by the diffractometer. For **4a**, **5b** and **8** the ω–2θ technique was used to measure reflections in the range $5 \leqslant 2\theta \leqslant 50°$ while for **4b** the ω technique was used. Three standard reflections (remeasured every 97 scans) showed no significant loss in intensity during data collection. The data were corrected for Lorentz and polarisation effects, and were corrected empirically for absorption. The unique data with $I \geqslant 3.0\sigma(I)$ were used to solve and refine the structures.

The structures of **4b**, **5b** and **8** were solved by direct methods while **4a** was solved by Patterson methods. All structures were developed by using alternating cycles of least-squares refinement and Fourier-difference synthesis. All non-hydrogen atoms were refined anisotropically, while all hydrogens were placed in idealised positions (C–H 0.96 Å) and assigned a common isotropic thermal parameter (U = 0.08 Å^2). Structure solution used the SHELXTL PLUS[36] program package on a microVax II computer. The final R and R' values together with residual electron density levels and other important crystallographic parameters are given in Table 7 which also gives data for **6b** and **7a**. Atomic coordinates for **4a**, **4b**, **5b**, **6b**, **7a** and **8** are listed in Tables 8–13 respectively.

Additional material available from the Cambridge Crystallographic Data Centre comprises H-atom coordinates, thermal parameters and remaining bond lengths and angles.

Acknowledgements

This work was supported by grants from the SERC (studentships to T. A. C. and G. D. F.), the Nuffield Foundation, the Royal Society of Chemistry and the University of London Central Research Fund.

References

1 See, for example, E. I. Stiefel, *Prog. Inorg. Chem.*, 1976, **22**, 1.
2 C. D. Garner and J. M. Charnock, in *Comprehensive Coordination Chemistry*, eds. G. Wilkinson, R. D. Gillard and J. A. McCleverty, Pergamon, Oxford, 1987, vol. 3, p. 1358.
3 See, for example, W. E. Newton, G. J.-J. Chen and J. W. McDonald, *J. Am. Chem. Soc.*, 1976, **98**, 5387; L. Ricard, C. Martin, R. Wiest and R. Weiss, *Inorg. Chem.*, 1975, **14**, 2300; L. J. de Hayes, H. C. Faulkner, W. H. Doub, jun. and D. T. Sawyer, *Inorg. Chem.*, 1975, **14**, 2110; J. Huneke and J. H. Enemark, *Inorg. Chem.*, 1978, **17**, 3698; K. S. Nagaraja and M. R. Udupa, *Transition Met. Chem.*, 1983, **8**, 191.
4 P. J. Baricelli, M. G. B. Drew and P. C. H. Mitchell, *Acta Crystallogr., Sect. C*, 1983, **39**, 843; S. Lu, M. Shang, W. Cheng, M. He and J. Huang, *Fenzi Kexue Yu Huaxue Yanjiu*, 1984, **4**, 435; M. G. B. Drew, P. J. Baricelli, P. C. H. Mitchell and A. R. Read, *J. Chem. Soc., Dalton Trans.*, 1983, 649.
5 A. W. Edelblut and R. A. D. Wentworth, *Inorg. Chem.*, 1980, **19**, 1110.
6 M. E. Noble, K. Folting, J. C. Huffman and R. A. D. Wentworth, *Inorg. Chem.*, 1983, **22**, 3671.
7 L. O. Atovmyan, V. V. Tkachen and S. A. Shchepinov, *Sov. J. Coord. Chem. (Engl. Transl.)*, 1978, **4**, 460.
8 K. L. Wall, K. Folting, J. C. Huffman and R. A. D. Wentworth, *Inorg. Chem.*, 1983, **22**, 2366.
9 M. E. Noble, J. C. Huffman and R. A. D. Wentworth, *Inorg. Chem.*, 1983, **22**, 1756.
10 A. W. Edelblut, B. L. Haymore and R. A. D. Wentworth, *J. Am. Chem. Soc.*, 1978, **100**, 2250.
11 J. Fletcher, G. Hogarth and D. A. Tocher, *J. Organomet. Chem.*, 1991, **403**, 345.
12 M. L. H. Green, G. Hogarth, P. C. Konidaris and P. Mountford, *J. Chem. Soc., Dalton Trans.*, 1990, 3781.
13 See, for example, I. S. Kolomnikov, Yu. D. Koreshkov, T. S. Lobeeva and M. E. Volpin, *Chem. Commun.*, 1970, 1432; E. A. Maatta, *Inorg. Chem.*, 1984, **23**, 2650; A. J. Nielson, *Inorg. Synth.*, 1986, **24**, 194.
14 P. Jernakoff, G. L. Geoffroy, A. L. Rheingold and S. J. Geib, *J. Chem. Soc., Chem. Commun.*, 1987, 1610.
15 J. C. Green, M. L. H. Green, J. T. James, P. C. Konidaris, G. H. Maunder and P. Mountford, *J. Chem. Soc., Chem. Commun.*, 1992, 1361.
16 V. C. Gibson, C. Redshaw, W. Clegg and M. R. Elsgood, *J. Chem. Soc., Chem. Commun.*, 1994, 2635 and refs. therein.
17 F. W. Moore and M. L. Larson, *Inorg. Chem.*, 1967, **6**, 998.
18 F. A. Schultz, V. R. Ott, D. S. Rolison, D. C. Bravard, J. W. McDonald and W. E. Newton, *Inorg. Chem.*, 1978, **17**, 1758.

19 T. A. Coffey, G. D. Forster, G. Hogarth and A. Sella, *Polyhedron*, 1993, **12**, 2741.

20 T. A. Coffey, G. D. Forster and G. Hogarth, *J. Chem. Soc., Chem. Commun.*, 1993, 1524.

21 G. D. Forster and G. Hogarth, *J. Chem. Soc., Dalton Trans.*, 1993, 2539.

22 G. D. Forster and G. Hogarth, *Polyhedron*, 1995, **14**, 1401.

23 W. A. Nugent and J. M. Mayer, *Metal-Ligand Multiple Bonds*, Wiley, New York, 1988.

24 J. Dirand-Colin, L. Ricard and R. Weiss, *Inorg. Chim. Acta*, 1976, **18**, L21; A. Müller, R. G. Bhattacharyya, N. Mohan and B. Pfefferkorn, *Z. Anorg. Allg. Chem.*, 1979, **454**, 118; B. Spivack, Z. Dori and E. I. Stiefel, *Inorg. Nucl. Chem. Lett.*, 1975, **11**, 501.

25 N. C. Howlander, G. P. Haight, T. W. Hambley, M. R. Snow and G. A. Lawrance, *Inorg. Chem.*, 1984, **23**, 1811.

26 L. Ricard, J. Estienne and R. Weiss, *Inorg. Chem.*, 1973, **9**, 2182; A. W. Gal, A. F. J. M. Van Der Ploeg, F. A. Vollenbrock and W. Bosman, *J. Organomet. Chem.*, 1975, **96**, 123; R. S. Herrick, S. Nieter-Burgmayer and J. L. Templeton, *J. Am. Chem. Soc.*, 1983, **105**, 2599; M. G. B. Drew, D. M. Williams and D. A. Rice, *Inorg. Chim. Acta*, 1984, **89**, L19; J. R. Morrow, J. L. Tonker and J. L. Templeton, *Organometallics*, 1985, **4**, 745; A. Mayr, G. A. McDermott, A. M. Dorries and A. K. Holder, *J. Am. Chem. Soc.*, 1986, **108**, 310; C. G. Young, M. A. Bruck, P. A. Wexler, M. D. Carducci and J. Enemark, *Inorg. Chem.*, 1992, **31**, 587; A. J. Deeming and R, Vaish, *J. Organomet. Chem.*, 1993, **460**, C8.

27 E. A. Maatta and R. A. D. Wentworth, *Inorg. Chem.*, 1979, **18**, 2409.

28 M. H. Schofield, T. P. Kee, J. T. Anhaus, R. R. Schrock, K. H. Johnson and W. M. Davis, *Inorg. Chem.*, 1991, **30**, 3595.

29 H. Alper, *Inorg. Chem.*, 1972, **11**, 976; W. H. Leung, G. Wilkinson, B. Hussain-Bates and M. B. Hursthouse, *J. Chem. Soc., Dalton Trans.*, 1991, 2791; B. Hansert and H. Vahrenkamp, *J. Organomet. Chem.*, 1993, **459**, 265; J. C. Bryan, A. K. Burrel, M. M. Miller, W. H. Smith, C. J. Burns and A. P. Sattelberger, *Polyhedron*, 1993, **12**, 769.

30 T. A. Manuel, *Inorg. Chem.*, 1964, **3**, 1703.

31 J. A. Jarvis, B. E. Job, B. T. Killbourn, R. H. B. Mais, P. G. O. Owston and P. T. Todd, *Chem. Commun.*, 1967, 1149.

32 W.-H. Leung, G. Wilkinson, B. Hussain-Bates and M. B. Hursthouse, *J. Chem. Soc., Dalton Trans.*, 1991, 2791; R. Hasselbring, H. W. Roesky and M. Noltemeyer, *Angew. Chem., Int. Ed. Engl.*, 1992, **31**, 601; W. A. Herrmann, G. Weichselbaumer, R. A. Paciello, R. A. Fischer, E. Herdtweck, J. Okuda and D. W. Marz, *Organometallics*, 1990, **9**, 489; P. Legzidins, E. C. Phillips, S. J. Rettig, J. Trotter, J. E. Veltheer and V. C. Yee, *Organometallics*, 1992, **11**, 3104.

33 G. Hogarth and P. C. Konidaris, *J. Organomet. Chem.*, 1990, **399**, 149.

34 J. Fletcher, G. Hogarth and D. A. Tocher, *J. Organomet. Chem.*, 1991, **405**, 207.

35 J. Dirand, L. Ricard and R. Weiss, *Transition Met. Chem.*, 1975, **1**, 2.

36 G. M. Sheldrick, SHELXTL PLUS, Program package for structure solution and refinement, version 4.2, Siemens Analytical Instruments Inc., Madison, WI, 1990.

Received 15th *February* 1995; *Paper* 5/00911A